Prince Edward Island

Coastal Hazards

July 2021

Report prepared for:
Province of PEI

Prepared by:
M.H. Davies, Ph.D., P.Eng.
N.J. MacDonald, Ph.D., P.Eng.

Contents

Figures

Tables

1 Introduction

This document presents the results of an assessment of coastal hazards along PEI's shores. This assessment is based on existing conditions as well as predictions of the future effects of climate change, most notably through a rise in relative sea levels.

1.1 Background

This study builds upon a strong foundation that has been developed in PEI for coastal mapping and hazard identification. The Province (largely through their work on the Atlantic Coastal Adaptation Solutions Project, ACASA) has amassed a substantial inventory of GIS maps and reports covering shore classification, historic erosion rates, sea level rise and storm criteria. Coldwater's participation in the ACASA project resulted in a shoreline classification GIS for the Province that includes a reach-by-reach description of shoreline type, bluff/bank height, nearshore wave climate, projected sea level rise, storm surge statistics and longshore sediment transport rates (Davies 2012).

These GIS datasets and tools have been used in conjunction with the latest projections of climate change and sea level rise to generate a probability-based risk assessment of coastal vulnerability.

Hazards (notably coastal erosion, storm damage and flooding) are described by both their probability of occurrence and their intensity. Methodology

Definition of coastal hazards involves the development of reliable, quantitative maps of coastal hazards – storm water levels, wave runup, sea level rise, tides, and erosion. Hazards are often assessed in terms of

the ‘exposure’ of a given site/property to a given hazard. In this case, since we are using GIS methods to create spatial maps of hazards, the sheltering effects of topography and bathymetry are taken into account in definition of the hazards. As such, exposure is integrated into the spatial definition of the hazards.

Hazard mapping allows identification, through spatial maps as well as summary tables, the spatial extent and severity of coastal hazards (flooding, storm damage and erosion) under both present-day conditions and future conditions based on projected climate change scenarios. This mapping allows identification of elements-at-risk – those infrastructure elements which are potentially exposed to coastal hazards.

The hazard mapping has been compared to documented damages and structural performance during recent storm events. This validates the analysis process and has guided refinement of the analysis techniques in order to obtain a high level of consistency between predictions and historical observations.

2 Coastal Hazards

To be able to describe coastal hazards a clear understanding is needed of the contributory factors. These include:

- Water levels
- Waves
- Erosion and sediment dynamics

One of the key challenges in coastal hazard work is to define the expected intensity and probability of occurrence of each of these hazards, as well as examining their interactions. Joint probability analysis is a key aspect of understanding the combined likelihood of occurrence of combinations of water levels, winds and waves. In some coastal environments, the response of the shoreline to ongoing and storm-related erosion processes can result in changes to the level of exposure at a site (e.g. dune erosion, overwash and barrier island erosion).

2.1 Flood Hazards

Coastal water levels result from a combination of mean water level, relative sea level rise, tides, atmospheric effects (barometric pressure, dynamic sea surface topography, surge), setup and wave action (wave impact, runup and overtopping). The latter of which are heavily influenced by shore geometry which can itself be shaped by tidal, wave and water level conditions.

There are three forms of coastal flooding:

- Direct inundation – the sea level exceeds the elevation of the land, this generally occurs on low coastal plains and in estuarine areas, and often occurs where waves have not built up a natural barrier such as a dune system.
- Barrier Overtopping – mean water levels remain below the coastal barrier (which may be either natural or man-made) and overtopping occurs due to wave runup heights exceeding the crest of the barrier, allowing water to flow over the top of the barrier, flooding the land behind it.
- Barrier Breaching – Wave-driven flows, wave impact and hydrostatic loading can cause failure of the barrier, allowing inland inundation.

Measures of flood intensity include water depth and duration, wave heights, runup, overtopping and flow conditions.

2.2 Erosion Hazards

One of the key challenges in addressing setbacks along coasts is to take into consideration the dynamic nature of the shoreline. In addition to flooding and wave damage, coastal hazards include erosion, and slope stability, as well as issues related to sediment dynamics (barrier breach, dune stability, and sedimentation). While this report highlights the implications of large-scale changes to coastal landforms such as barrier islands, a significant research effort is needed to better understand and quantify these processes.

2.3 Defining the hazard

Relative sea level rise, storms, rainfall, runoff, river flow and tsunamis can all factor in the frequency and severity of flood events. The present analysis is limited to floods caused by sea levels and storm waves – the effects of tsunamis and rainfall/runoff events are not considered.

Coastal flooding is expected to become more frequent and severe in PEI as well as many other areas of Canada due to local sea level rise (Bush & Lemmen 2019). Relative sea level change is due to a combination of land subsidence (or uplift) and global sea level rise and adds to the challenge of predicting future coastal flood hazards. James et al (2014) provide a detailed analysis of the effects of rising global sea levels, and changing land elevations (predominantly due to glacial isostatic adjustment) on local sea level change in Canada.

The coastal flood hazard varies both spatially and temporally. The tidal range around PEI (HHWLT to LLWLT) varies by almost a factor of three, from as small as 1.0 m on the north shore near Tracadie, to as large as 2.9 m near Charlottetown.

Storm surges can cause short-term increases in sea levels by up to 1.5 m. Storm surge patterns tend to linearly increase from north to south with the largest surge amplitudes being observed along the south shore. The variation in surge magnitude is much smaller than the tidal variation. Surges on the north shore are typically 90-95% of that on the south shore.

Along the north shore, storms can generate waves over six metres high while waves of 1 to 3 metres are more common in the waters of Northumberland Strait.

One of the key challenges in defining coastal hazards is the accurate determination of the probabilities of occurrence of combinations of sea levels, tides, storm surges and waves at any given site around the Island.

2.4 Flood Hazard Delineation

Table 2-1 (Shrubsole, et al. 2003) shows that under the former federal Flood Damage Reduction Program (FRDP), British Columbia used a 200-yr return period flood event, while the rest of Canada used a 100-yr return period, also known as the 1% Annual Exceedance Probability (AEP). Logically, it is consistent to base coastal flood hazard assessments on the same approach used for inland waters. Hence the 100-yr flood (1%AEP) forms the basis for our coastal flood hazard delineation.

Historically, a fixed standards-based approach has been used for addressing natural hazards in Canada, where floodplains elevations are based on one specific design flood (typically for the 1% or 0.5% AEP). This approach does not address the full range of potential flood events, where high frequency/low impact flooding may lead to cumulative impacts, or where rare but severe floods may lead to worse impacts than those experienced under the design flood.

International best practices are shifting towards a risk-based or risk-informed approach to flood hazards (Sayers et al. 2013). Rather than focussing on a single event, using a broader approach that considers what is at risk and then maximizes social, economic and environmental benefits under a range of flood scenarios. This approach moves away from a 'one size fits all' approach and instead allows evaluation of sites and infrastructure based on both the range of hazards possible and the potential consequences of a flood event.

The National Research Council has recently produced a frst edition of *Coastal Flood Risk Assessment Guidelines for Building and Infrastructure Design* (Murphy, et al. 2020) which provides a broad framework for addressing coastal flood risk assessments in Canada.

Province/ Territory	Communities	Number Mapped	Number Designated	Regulatory Flood	Definition of Floodway
B. C.	143	77	73	1:200	See Note 1
Alberta	67	20	11	1:100	Hydraulic (2)
Sask.	24	22	16	1:500	Hydraulic (2)
Manitoba	26	18	16	1:100	Hydraulic (2)
Ontario	445	318	211	See Note 3	1:100
Quebec	510	211	24	1:100	1:20
N. B. (4)	15	12	12	1:100	1:20
N. S.	6	6	5	1:100	1:20
P. E. I. (4)		0	0		
Nfld. & Labr. (4).	53	19	16	1:100	1:20
Yukon		0	0		
NWT	9	9	9	1:100	Hydraulic (2)
Nunavut	0	0	0	1:100	Hydraulic (2)

Modified from: Watt (1995); Kallio (2001)

Notes:

1. The floodway in British Columbia is defined as the natural channel width plus a minimum 30 m setback.
2. The hydraulic floodway uses criteria of less than 1.0 m/s velocity, less than 1.0 m depth and no more than 0.3 m rise.
3. Ontario's regulatory flood uses the Hurricane Hazel rainfall, the Timmins storm, and the 100-year flood elsewhere.
4. The Atlantic Provinces may also use a historic event or flood from a specified input, provided the water levels are higher than those of a 100-year flood.

Table 2-1 Regulatory flood criteria for Canadian Provinces (Shrubsole et al, 2003)

2.5 Mapping the hazard

Coastal flood hazard assessments have traditionally been 'profile-based', in which nearshore wave transformation, wave runup and flood elevation are determined on representative cross-shore profiles. This analysis develops flood elevations which are then applied on a reach-by-reach basis along the shore (e.g. Ontario MNRF, 2001, British Columbia, 2012, FEMA 2015).

As field datasets and computational tools improve, the use of 2D process-based analysis and mapping is becoming more widespread.

LiDAR-derived digital elevation models (DEMs) are the basis for GIS-based floodplain mapping. There are three typical approaches to floodplain mapping using DEMs:

- Static topographic mapping – treating the flood hazard as a constant elevation and mapping that elevation along the shore. All elevations below the flood level are mapped as within the floodplain regardless of hydraulic connection (sometimes referred to as 'bathtub modelling').
- Hydro-enforced mapping - modifications are made to the DEM; bridge decks and road fills at culverts are 'cut through' to create hydraulic pathways. Flooding is then allowed to propagate from open water inland using these flow pathways.
- Hydro-modelling – this involves the use of hydrodynamic models to simulate flows through culverts and streams to capture the flow dynamics of flood propagation.

Static mapping has been undertaken previously by the Province for some communities using present-day and future sea level scenarios combined with a 1%AEP flood level as proposed by Richards & Daigle (2011). This mapping used a horizontal flood surface for each map with no consideration of wave effects. This approach provides a quick and effective visualization of potential flood areas.

Hydro-enforced mapping has not been extensively used in PEI but is a common technique in other jurisdictions. This approach provides increased detail and more realistic inundation mapping at a cost of the effort to modify the DEMs.

Hydrodynamic modelling for flood mapping is generally restricted to specific problem areas or as research projects. This approach requires detailed analysis of bathymetry and flow conditions and is typically only used over relatively small domains. An example of this approach is Bridgewater, NS (Webster, McGuigan and Collins, et al. 2014), where the DHI model MIKE-Flood was used to simulate and map combined river and tidal flows.

The choice of approach taken for floodplain mapping depends on the spatial extent of the study area, the desired resolution of the mapping, and the types of flooding mechanisms to be included.

The Federal Flood Mapping Framework (Natural Resources Canada 2018) identifies four main types of flood map:

- Inundation Maps (showing floodwater coverage for flood events of differing magnitudes)

- Flood Hazard Maps (showing the extent of a regulatory design flood for land use planning and flood mitigation)
- Flood Risk Maps (flood hazard maps that incorporate socio-economic values such as potential loss or property vulnerability), and
- Flood Awareness Maps (poster-styled maps for public information).

The recently released federal guidelines for floodplain mapping (Natural Resources Canada 2019) includes some guidance for coastal hydrodynamics for mapping of coastal floodplains.

Along highly-developed coastlines, the empirical estimation of wave runup remains the tool of choice for assessing wave effects during coastal storms (e.g. (van der Meer, Bruce, et al. 2018), (Melby 2012)). In coastal areas with minimal development, particularly in areas where low coastal plains get inundated during extreme flood events, comprehensive two-dimensional wave/setup models can be used. CMS-Wave, Mike21 and SWAN are examples of spectral wave models that combine sophisticated wave transformation modelling with wave setup and inundation modelling. Two-dimensional modeling and wide-area, high resolution digital elevation models (typically LiDAR-based) have enabled the development of two- and three-dimensional flood plain mapping techniques. The CMS-Wave predicts coastal inundation (including the effects of wave set-up) and estimates wave runup on open shores as a function of wave height at the shore (Lin, Demirbilek, et al, 2008 and Li, Lin and Burks-Copes, 2012). In Canada, this technique has been applied for coastal flood hazard mapping in Lake Erie (Shoreplan, 2010).

LISFLOOD-FP (Bates et al, 2015) is a two-dimensional hydrodynamic model specifically designed to simulate floodplain inundation in a computationally efficient manner over complex topography. It is capable of simulating grids up to 10^6 cells for dynamic flood events. The model predicts water depths in each grid cell at each time step, and hence can simulate the dynamic propagation of flood waves over fluvial, coastal and estuarine floodplains. This is a non-commercial, research code that is focussed on channel and floodplain flows and does not address the effects of wave action.

The SWAN model (The SWAN Team 2009) predicts nearshore inundation by storm water levels, including wave setup as well as predicting wave conditions for flooded areas. Coastal flood hazard delineation with the model can be applied directly in inundated open

beach areas (Slinn 2008), or can be coupled to empirical runup predictors for steeper, non-inundated shorelines (Vitousek, et al. 2009).

The focus of the work in the present study is coastal floodplain mapping to allow evaluation of infrastructure vulnerabilities and to explore mitigation opportunities. The Federal Geomatics Guidelines for Flood Mapping has not been released at the time of undertaking this study. It is expected to provide useful guidance that would shape any final (regulatory) mapping products.

The delineation of the vertical elevations and horizontal setbacks that constitute the coastal flood hazard requires the following steps:

1. Establish local mean sea level over the planning timeframe (present-day to, say, 2100).
2. Define statistics of extreme water levels at the site (addressing the joint probabilities of tides and storm surges).
3. Determine nearshore wave conditions (including wind- and wave-driven setup).
4. Wave modelling to include definition of the wave envelope and wave runup effects.
5. Define inundation and wave impact zones

2.6 Methodology

For the present study the focus is on generating comprehensive mapping of the entire province at the finest practical spatial resolution. Particularly on the north shore of PEI, the effects of waves are an important aspect of coastal flooding. The SWAN model was selected to address nearshore wave conditions as well as the increases in coastal water levels due to wave breaking (wave set-up) and the inundation of low-lying coastal lands.

The following steps were undertaken in this analysis:

- Develop joint-probability tide-surge distributions and determine still water levels (SWLs) for present-day and future relative sea level rise scenarios.
- Analyze offshore waves (from the MSC-60 wave hindcast) and model nearshore wave transformations and wave setup using SWAN for the 2010 and 2100 1% AEP water levels and wave conditions.

- Determine waves heights, flood water levels (TWLs) and base flood elevations (BFE) from the SWAN results.
- Develop inundation maps using hydro-enforced DEM and (regionally-averaged) TWLs to generated Flooding Maps (TIF format to match all DEM footprints).
- Project wave conditions onto shoreline vector along with cross-linkages to TIF, Hs and BFE files.

Following evaluation of patterns in the spatial variability of the resulting coastal flood hazards, the mapping was simplied to provide consistent flood elevations on a watershed-by-watershed basis. This involved mapping the results of the inundation mapping onto each of the 287 watersheds delineated by the Province. Each of these watersheds terminates at the sea or major bay/estuary.

3 Technical Analysis

Water levels are the main criteria for coastal flooding (although, as will be discussed later, wave conditions, flow rates and velocities can also be important). Water levels vary on several time scales varying from seconds (in the case of waves) through to seasonal and decadal variations.

Wind-generated waves have periods of between 1 and 20 seconds. Wave heights in the open Gulf of St. Lawrence can have significant wave heights as high as H_s =6 m*. Storms can last from a few hours up to several days.

The energy released by wave breaking creates variations in water levels throughout the surf zone, with a reduction in water levels (set-down) near the break point and an increase in water levels (set-up) near the shore. For typical storm conditions, wave setup is 7 to 8% of the offshore wave height (Dean, et al. 2005), so with offshore waves with H_s =3-5m, wave setup can increase water levels at the shore by 0.20 to 0.40 m.

Tides cause variations in water levels on time scales varying from hours to years. While the dominant tidal pattern around PEI is a semi-diurnal tide (6.2 hours from high tide to low tide), tidal patterns vary in response to the motions of the sun, the moon and other planets seasonal and decadal variations in tidal heights.

Coastal flood hazard mapping requires evaluation of all of the contributing factors to flood conditions, namely:

- Mean sea levels
- Relative sea level rise due to climate change
- Tides
- Storm water levels
- Waves

This section of the report describes the approaches taken to evaluate these factors.

* The significant wave height, H_s is a common measure of the representative wave height. It is the average height (crest-to-trough) of the 1/3 highest waves in a sea state. The largest wave, H_{max} is typically 1.6 to 1.8 times higher than H_s, the average wave , $\overline{H}$ is typically 0.6 H_s.

3.1 Datums

The use of datums (vertical reference planes) and the term 'mean sea level' can lead to confusion when dealing with coastal flooding. The following provides some context into the various datums commonly in use and how to move between them.

In an idealized global ocean without tides, water density variations, currents or weather, the sea surface would follow an equipotential surface, with no flows and with the surface uniformly perpendicular to the force of gravity. This undisturbed equipotential surface, the *geoid*, forms our key reference datum for determining vertical elevations. Until 2013, the term 'geodetic datum' in Canada generally referred to the Canadian Geodetic Vertical Datum of 1928 (CGVD28) which was an approximation of mean sea level circa 1928, based on water level records at several gauge sites. In 2013, Natural Resources Canada released a new national geodetic datum, CGG2013, which is a more sophisticated, detailed and up-to-date estimation of mean sea level. It is an equipotential gravitational surface which represents by convention the coastal mean sea level for North America (www.nrcan.gc.ca/earth-sciences/geomatics/geodetic-reference-systems). This geoid is expressed as a gravitational equipotential, W_o=62,636,856 m^2/s^2.

The vertical separation between the CGG2013 and CGVD28 datums vary spatially across Canada, for example, the CGG2013 datum is 15cm below CGVD28 at Vancouver and 64cm above it at Halifax. Furthermore, while CGG2013 represents 'by convention' mean sea level, actual mean water levels deviate quite a bit from CGG2013. The sea's mean water level at Vancouver is 19cm above CGG2013, while the mean water level at Halifax is 39cm below it. This difference is due to variations in dynamic sea surface topography (effects of atmospheric pressure, water density and current patterns, etc. that cause the mean sea surface to vary).

Floodplain topography and elevations of buildings and infrastructure are generally mapped relative to geodetic datum, whereas bathymetric and tidal gauge data is typically reported relative to the local datum of hydrographic charts (Chart Datum, which is usually defined based on a low tide reference derived from water level records at a local tide gauge). The use of Chart Datum for bathymetric data can create challenges when conducting large-scale regional assessments of coastal flood hazards, which can encompass areas where bathymetric data is referenced to different local Chart Datums.

Care must be taken in ensuring that appropriate and consistent datums are being used in considering flood hazards and that the correct datum conversions are being applied. This is compounded by the fact that anecdotally both CGVD28 and CGG2013 are referred to as 'geodetic datum' or even 'mean sea level'. In this document, the term Mean Sea Level (MSL) refers to the local mean sea level as per hydrographic convention (IHO 2011)[†], not the geodetic mean sea level.

Efforts have recently been made to simplify datum conversions for hydrographic applications in Canada through the development of Hydrographic Vertical Separation Surfaces (HyVSEPs) (Robin, et al. 2016). These are surfaces that capture the spatial variability of tidal datums and levels using the geoid model, semi-empirical models, dynamic ocean models, satellite altimetry, relative sea level rise estimates, and tide gauge observations. HyVSEPs facilitate direct conversion between hydrographic elevations (chart datum, tidal elevations, mean sea level) to geodetic elevations (CGG2013). However, care should be taken when applying the surfaces, considering the many assumptions and uncertainty associated with models on which the surfaces are based, and local discrepancies with datum offsets at tide gauge sites and in areas where tides are affected by river flows, and/or shallow nearshore bathymetry. Natural Resources Canada's GPS-H software allows conversion between CGVD28, CGG2013 and GPS-derived ellipsoid elevations (Natural Resources Canada, 2019). More detail on use of HyVSEPs is given in Section 3.4 of this report.

For this report, much of the input data pre-dates the CGG2013 datum and is reported relative to CGVD28. The flood plain mapping undertaken in this report uses CGG2013 except where noted otherwise.

3.2 Mean Sea Level

Regression analysis shows that the rate of sea level rise in Charlottetown has been steady at 0.321 m/century over this period (3.21 mm/yr). As this data shows, mean sea level data is inherently noisy, with variations of ±10 cm year-to-year due to changes in weather patterns and oceanic circulation. While climate change modelling predicts a marked increase in the rate of sea level rise as the world adjusts to increased levels of greenhouse gasses, the noise in the observed sea level data makes it

[†] IHO 2011 reads: Mean Sea Level: The average HEIGHT of the surface of the SEA at a TIDE STATION for all stages of the TIDE over a 19-year period, usually determined from hourly height readings measured from a fixed predetermined reference level (CHART DATUM).

difficult to detect any acceleration in the rate of sea level rise as of 2015. The issue of observed and projected sea level rise is addressed in the IPCC's 5th Assessment Report – WGI Chapter 3 (Intergovernmental Panel on Climate Change, 2015). While there is some evidence from global datasets that the rate of sea level rise is increasing, the effect to date at Charlottetown is almost imperceptible. This does not necessarily contradict predictions of future sea levels due to climate change; it does however highlight the uncertainties involved in predicting the magnitude of expected sea level rise and the associated timing of that rise.

REGRESSION ANALYSIS: Monthly mean water levels from CHS Gauge 1700 (Charlottetown, PE)

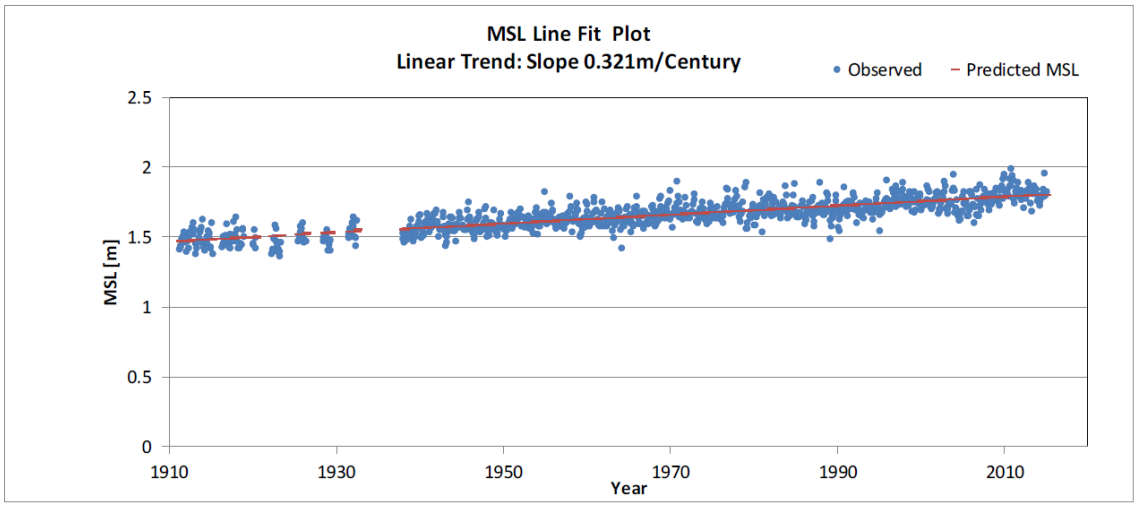

Regression Statistics	
Multiple R	0.8282
R Square	0.6859
Adjusted R Square	0.6856
Standard Error	0.0615
Observations	1048

ANOVA

	df	*SS*	*MS*	*Significance F*
Regression	1	8.6418	8.6418	2.8935E-265
Residual	1046	3.9580	0.0038	
Total	1047	12.5998		

	Coefficients	*Standard Error*	*t Stat*	*P-value*	*Lower 95%*	*Upper 95%*
Intercept	-4.670	0.132	-35.292	0.000	-4.929	-4.410
MSL	0.00321	0.00007	47.78954	0.00000	0.00308	0.00334

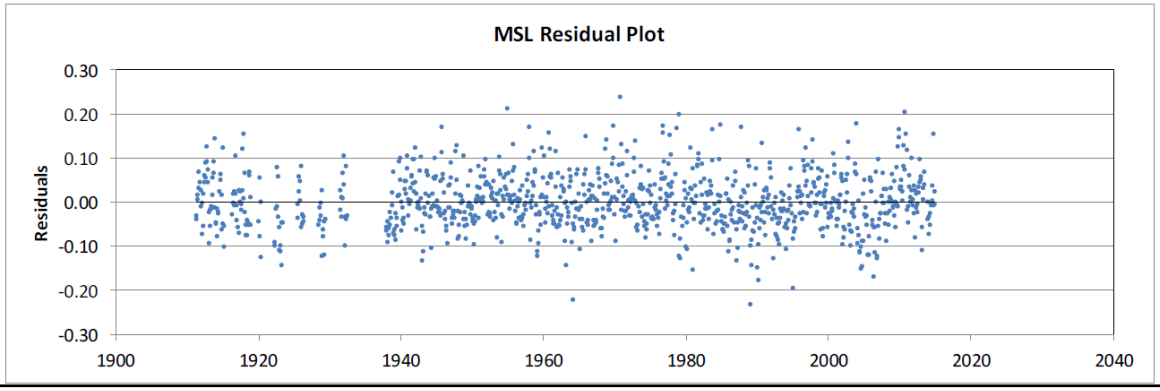

Figure 3-1 Sea level rise measurements – Charlottetown

3.3 Effects of climate change on sea levels

With climate change, sea levels are expected to increase significantly in the future, increasing coastal flood and erosion hazards. Natural Resources Canada (James, Henton, et al., Relative Sea-level Projections in Canada and the Adjacent Mainland United States 2014) presents detailed predictions for sea level rise for specific locations around Canada and adjacent US states. These projections are based on the Representative Concentration Pathway (RCP) scenarios of the Fifth Assessment Report of the Intergovernmental Panel on Climate Change (IPCC AR5). They include contributions from the thermal expansion of the ocean, glacial melting and discharge, anthropogenic influences and local crustal movements (e.g., crustal subsidence and post-glacial isostatic rebound).

The RCP scenarios were developed for the climate modelling community to integrate work being performed by research organizations around the world. The four scenarios are shown graphically in Figure 3-2 and can be summarized as follows (van Vuuren, et al. 2011):

- The RCP2.6 scenario is reduction scenario in which greenhouse gas concentrations peak around mid-century, then fall to low levels by 2100. Its development was based on approximately 20 published scenarios.
- The RCP4.5 scenario is a stabilization scenario in which greenhouse gas concentrations is stabilized shortly after 2100, without overshooting the long-range targets. It takes an intermediate approach to both emissions and mitigation efforts. Its development was based on 118 published scenarios and describes most of the scenarios published world-wide.
- The RCP6 scenario is a stabilization scenario in which greenhouse gas concentrations is stabilized shortly after 2100, without overshooting the long-range targets. It is very similar to RCP4.5 but assumes different mitigation efforts. Its development was based on approximately 10 published scenarios.
- The RCP 8.5 scenario is based on increasing greenhouse gas emissions over time and is a high emission scenario. Its development was based on approximately 40 published scenarios.

While RCP4.5 may arguably describe the most probable sea level rise scenario according to present research, recent emissions track closely to RCP8.5 (Zhai, Greenan, et al. 2014) and the incorporation of the upper end of the range in RCP8.5 may be more relevant to management and

planning in coastal areas (James, Henton, et al., Relative Sea-level Projections in Canada and the Adjacent Mainland United States 2014). Furthermore, at Charlottetown the median value of the RCP8.5 scenario sea level rise (0.728 m) falls within the 5%-95% range for RCP4.5 (0.29 m to 0.82 m). Therefore, RCP8.5 scenario was adopted for use in the present work to for future sea level scenarios.

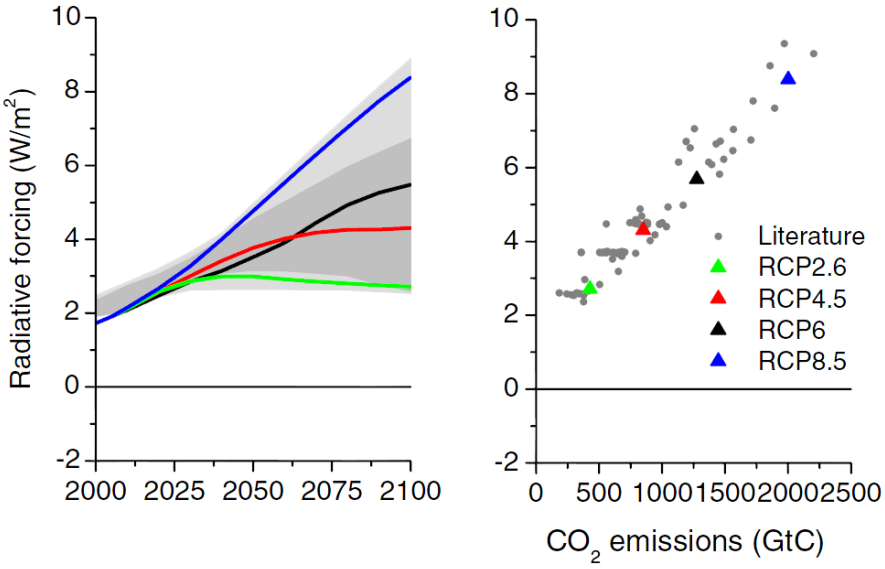

Figure 3-2 Characteristics of the four RCP plans (van Vuuren, et al. 2011)

Rising relative sea levels can increase both the severity and frequency of floods. The annual exceedance probabilities for different water levels in Charlottetown Harbour under present-day and projected future sea levels (median estimate RPC8.5) are shown in Figure 3-3. Predicted mean sea levels in 2045 are expected to exceed today's level by approximately 20 cm; by 2090, levels are expected to be 62 cm higher than today. Presently, a water level of 4.25m above chart datum – high enough to flood much of the waterfront – has a 1% chance of occurring in any given year; by 2045, the probability of such an event will have risen to 2.5% and, by 2090, an event of this magnitude has a 20% chance of occurring in any given year. These estimates do not include considerations for potential future changes in climate variability or the frequency and intensity of storms (e.g. Barnard et al. 2015), modification of storm surges and tidal ranges due to changes in water depths (locally and globally) (e.g. Schindelegger et al. 2018), or the nodal modulation of tides over decadal timescales that dominates mean annual tidal ranges on the east coast (Houston & Dean 2011).

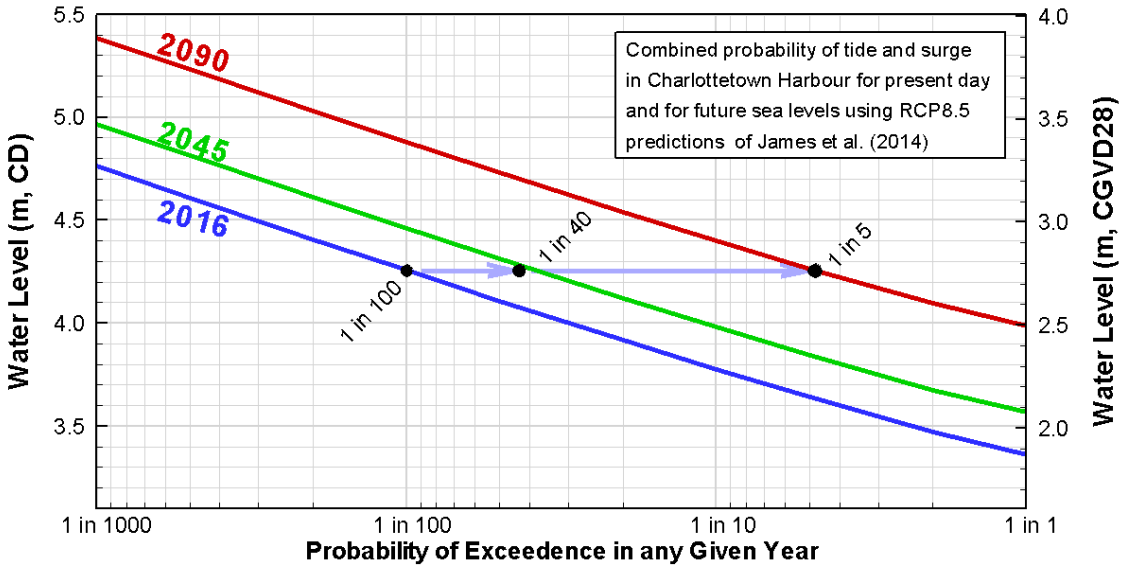

Figure 3-3. Probability of encountering high water levels (tide + storm surge) in selected years

3.3.1 Upper Bound Sea Level Rise

In 2016 DFO published an additional sea level rise guidance for Canadian waters (Han, et al. 2016) which is as much as 1m higher by 2100 than the more broadly accepted guidance presented in James et al (2014). The CAN-EWLAT site continues to focus on the James et al values but does reference the higher levels of the Han et al report as an upper bound for consideration. These new, higher, projections follow the upper bound sea level scenarios presented by NOAA (Sweet, et al. 2017). Jevrejeva et al (2014) estimate that sea level rises larger than 1.80m are less than 5% probable based on a probability density function of global sea level at 2100. The James et al (2014) sea level scenarios have been used in the present analysis.

3.4 HyVSEPs

NRCAN and DFO have developed a set of Hydrographic Vertical Separation surfaces (HyVSEPs) for the tidal waters of Canada (Robin, et al. 2016)[‡]. These surfaces provide a continuous mapping of the spatial variability of the tidal datum and tide levels between tide gauges and the offshore. The HyVSEPs provide a vital linkage between hydrographic surfaces (chart datum and tidal ranges), mean sea level, and geodetic datums such as CGVD28 and the newer CGG2013.

[‡] Point data from the HyVSEP surfaces is accessible through the CAN-EWLAT website.

Figure 3-4 shows an example application of data from the HyVSEP geodetic database – in this case, a subset of the dataset showing the vertical separation between hydrographic chart datum (CD) and the new 2013 national geodetic datum for PEI coastal waters.

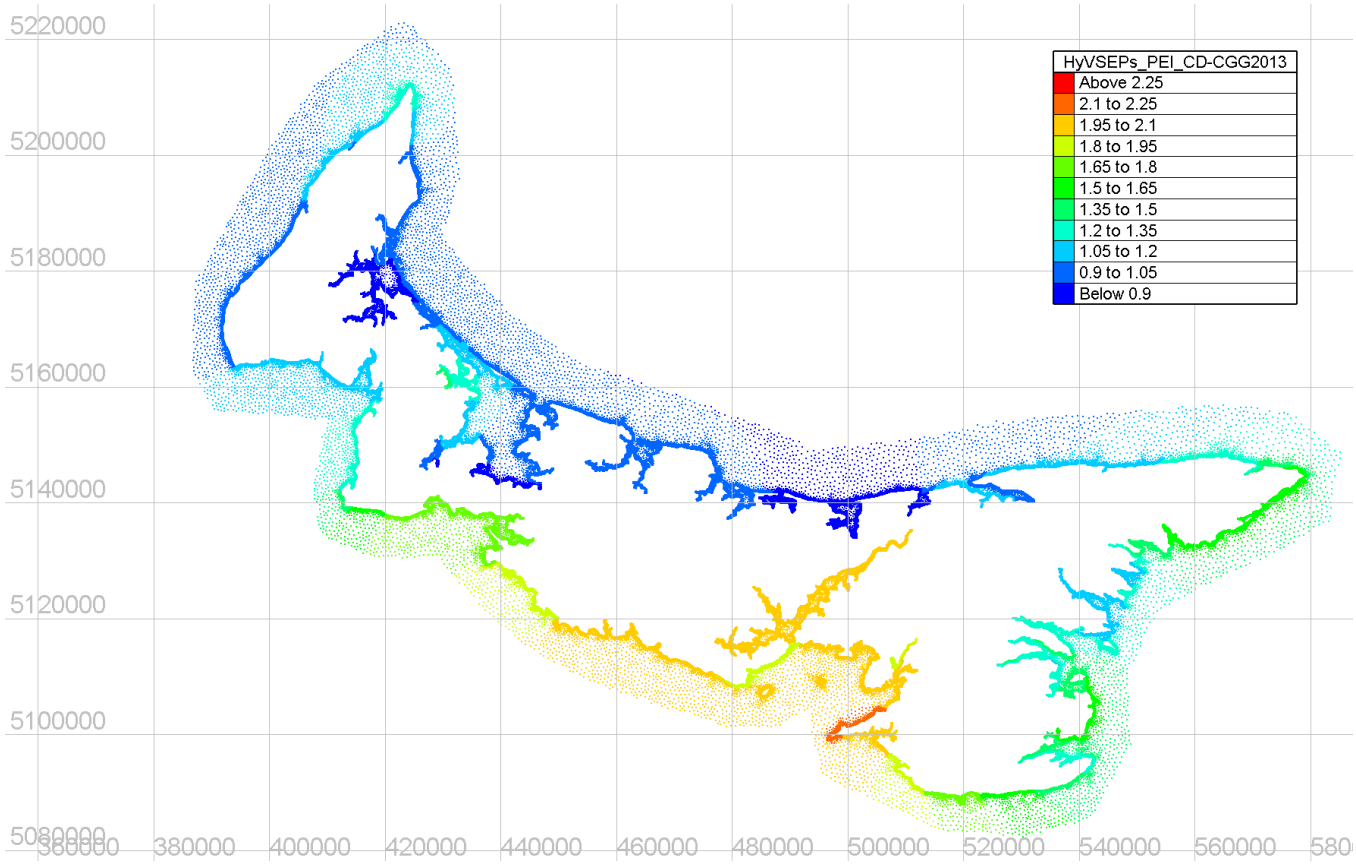

Figure 3-4 NRCAN HyVSEP Geodetic surface of the elevation of CGG2013 above Chart Datum

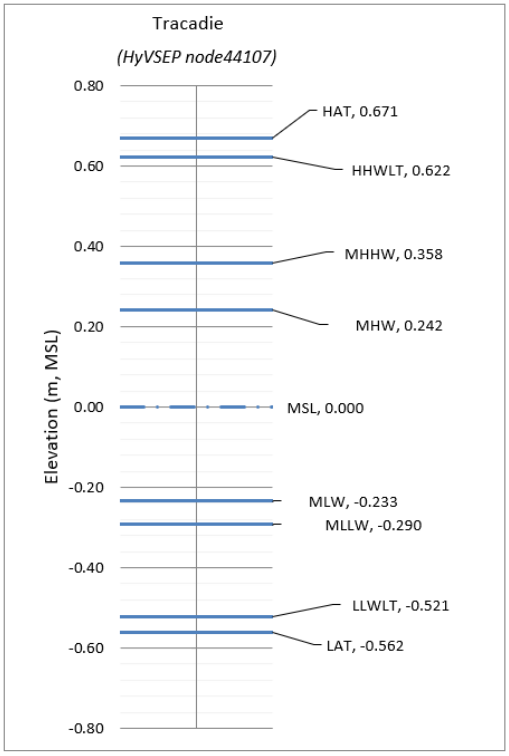

Figure 3-5 Tide levels at Tracadie relative to MSL (HyVSEP)

Table 3-1 HyVSEP data for Tracadie giving tidal elevations in various datums

44107	HAT	HHWLT	MHHW	MHW	MSL	MLW	MLLW	LLWLT	LAT
CD	1.192	1.143	0.879	0.763	0.521	0.288	0.231	0.001	-0.041
CGVD28	0.656	0.606	0.343	0.227	-0.016	-0.249	-0.306	-0.536	-0.578
CGG2013	0.324	0.275	0.011	-0.105	-0.347	-0.580	-0.637	-0.868	-0.909
MSL	0.671	0.622	0.358	0.242	0.000	-0.233	-0.290	-0.521	-0.562

3.5 Tides

Tides cause variations in water levels on timescales varying from hours to years. While the dominant tidal pattern around PEI is a semi-diurnal tide (6.2 hours from high tide to low tide), tidal patterns vary in response to the motions of the sun, the moon and other planets. Quadrature with the sun and moon creates a 14-lunar day tidal pattern known as spring-neap tides. Spring (largest) tides occur near the new and full moons when the gravitational pulls of the sun and the moon are aligned.

The elliptical shape of the moon's orbit around the earth leads to larger tides when the moon is in perigee (closest to the earth), which occurs every 27.6 days. When a new or full moon coincides with perigee this results in unusually large tides known as perigean spring tides, which occur 3 or 4 times a year.

Tides are further increased when the earth is closest to the sun (perihelion) which occurs in the first week of January (two weeks after the winter solstice). Perigean tides occurring near the time of perihelion lead to the highest tides of the year. These are sometimes referred to as “King tides”.

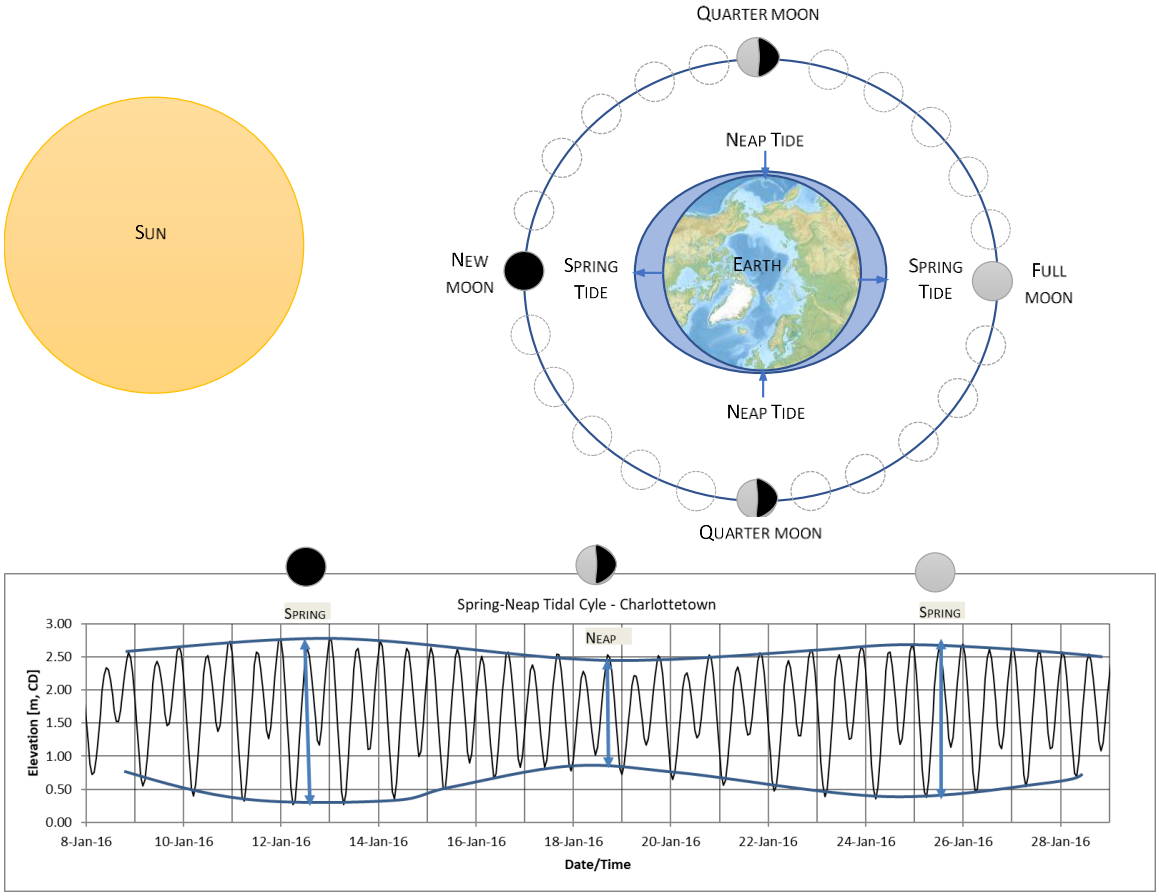

Figure 3-6 Spring-Neap tide cycles

Figure 3-7 shows the distribution of monthly maximum astronomic tides at Charlottetown over a 100-year period from 1950 to 2050. This figure is presented in boxplot format, where the box extends from the lower to upper quartile values of the data, with a line at the median. The whiskers extend from the box to show the range of the data. The scatter points show the individual maxima. This figure shows that peak monthly tides vary from a low of 1.1 (above MSL) in June to a peak of 1.23 in January, corresponding to the afore-mentioned ‘King’ tides. The actual timing of King tides varies year-to-year depending upon how close perigee and perihelion are to coinciding. King tides therefore sometimes occur in late December, sometimes in early January.

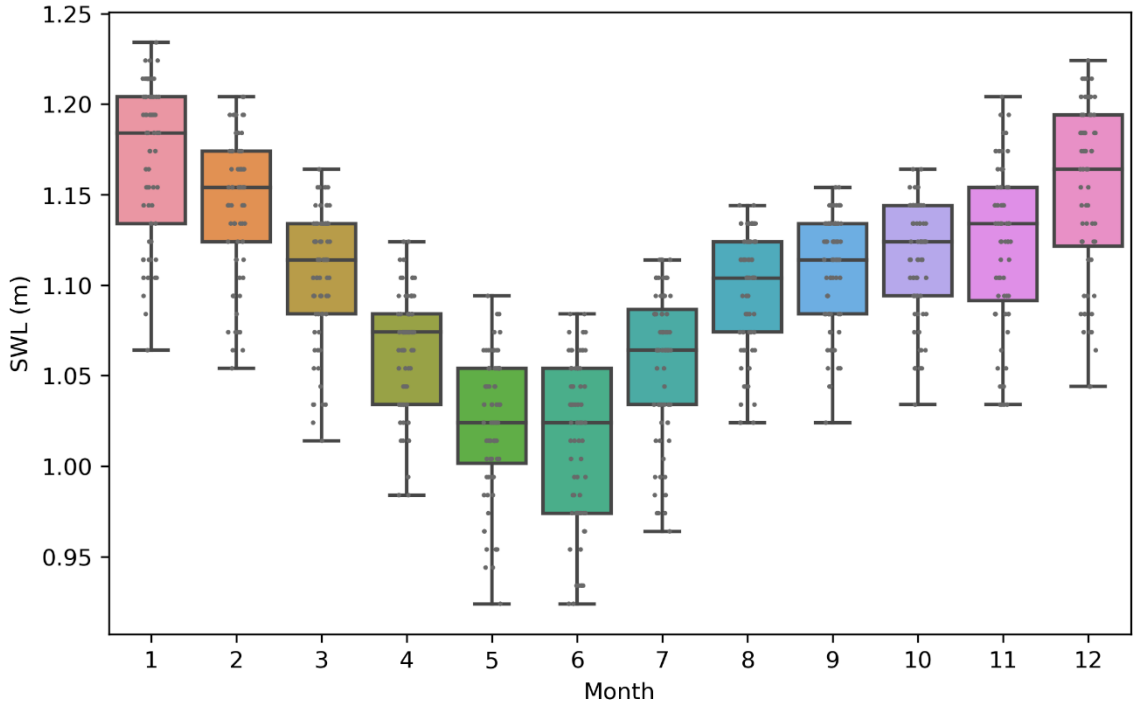

Figure 3-7 Seasonal variations in the monthly maximum astronomic tide at Charlottetown

The relative positions of the earth, moon and sun repeat themselves every 18.6 years – the Draconic cycle. At Charlottetown, for example, the monthly maximum astronomical tide is plotted over the 100-year period from 1950 to 2050, shows the rhythmic pattern in peak tide heights corresponding to the Draconic cycle (Figure 3-8). The dashed line in this figure is a fitted sine curve with a period of 18.6 years to illustrate the Draconic cycle`. The amplitude of this variation is, however, just 5cm and as such, not a major factor in peak water levels.

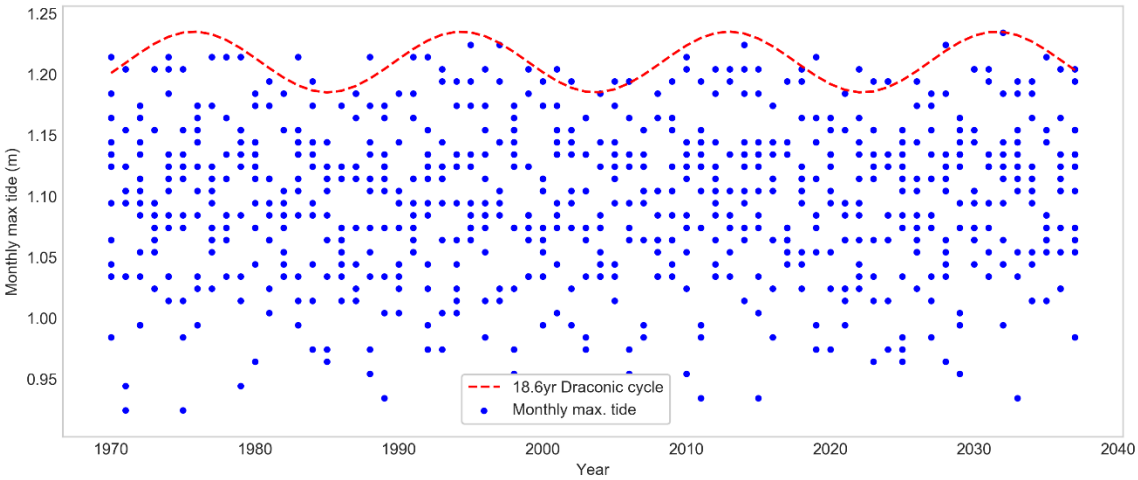

Figure 3-8 Saros cycle at Charlottetown

Tidal ranges (from high tide to low tide) vary by more than a factor of two around the Island. As shown in Figure 3-9, the tidal range along the north shore is between 1 and 1.4m, while in the Charlottetown area the range is over 2.8m. This is due to the way the tides propagate in the Gulf of St. Lawrence and then wrap around the Island to meet (doubling up) in Hillsborough Bay.

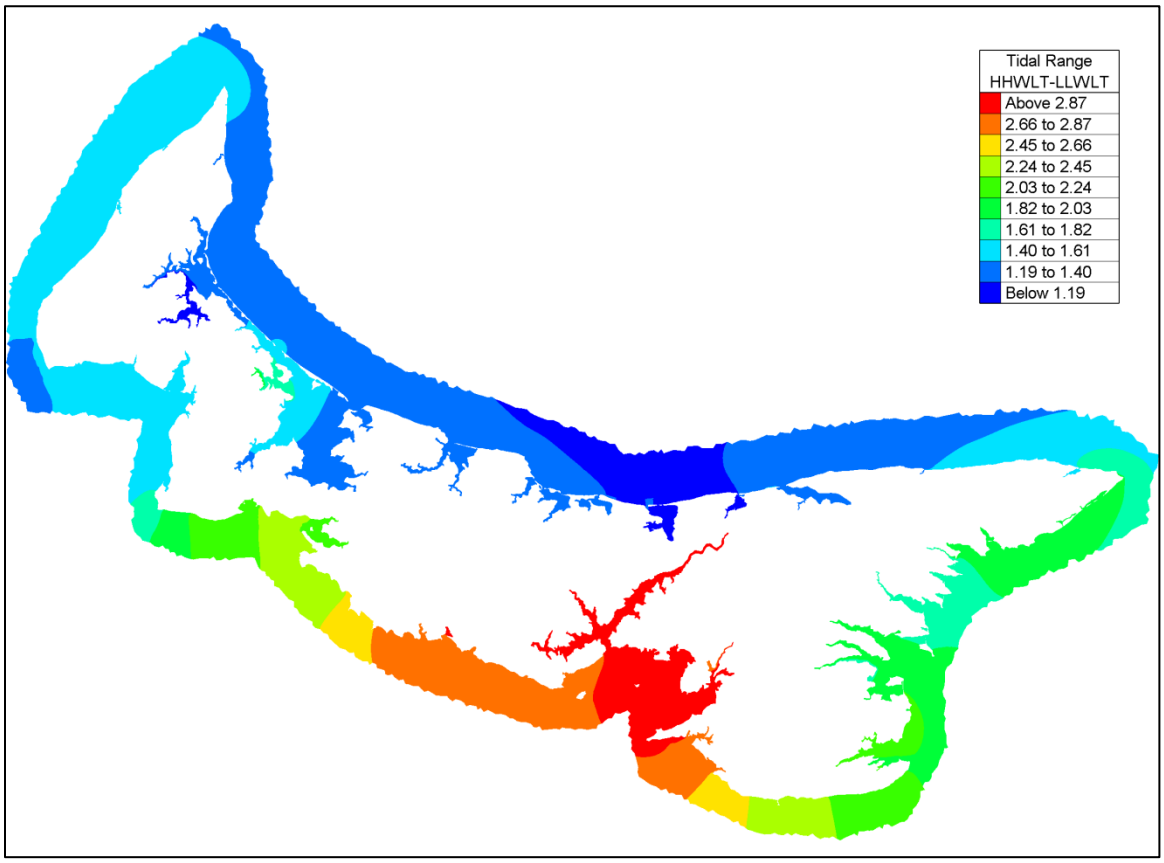

Figure 3-9 Tidal range

3.6 Storm surge

Storm surge is the increase in water levels above tidal level caused by the combined effects of barometric pressure drops and winds. The most extreme storm surge on record for the Island is the Charlottetown storm of January 21st, 2000 when a 1.3 m storm surge caused peak sea levels to rise to 4.23 m above chart datum.

Storm surge data can be derived from water level records at tidal gauges, from operational storm surge forecast models of from hindcasting models.

Analysis of surge statistics from observed water level (tide gauge) measurements has been traditionally performed by computing the 'residual' – the instantaneous elevation difference between the

observed water level and the expected astronomic tide as predicted by harmonic analysis. Figure 3-10 shows two weeks of water level data for Charlottetown from the Fisheries and Oceans Canada data archive[§]. The water level at any given point in time can be broken down into the following components:

$$\eta_{TWL} = \eta_{Tide} + \eta_{Surge} + \eta_{RSL}$$

Where η_{TWL} is the total water level, η_{Tide} is the water level due to astronomic (normal) tides, η_{Surge} is the superelevation of the water level due to surge, and $\eta_{RSL}$is the contribution from relative sea level rise which is the combined effects of sea level rise and land subsidence.

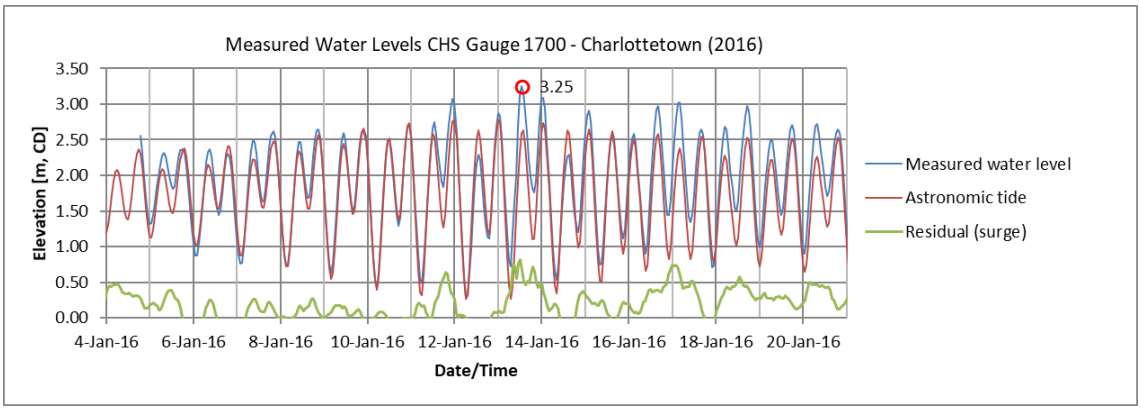

Figure 3-10 Sample of measured water levels at Charlottetown.

As noted in Haigh et al (2016), while the non-tidal residual primarily consists of the surge, it may also contain harmonic prediction errors, timing errors and non-linear interactions. Recently researchers (Williams, et al. 2016, Wahl and Chambers 2015) have been advocating the use of the 'skew surge' statistic which is the difference between the maximum observed sea level and the predicted (astronomical) tidal level, regardless of their timing during the tidal cycle. The skew surge has been shown to be independent of tide for large events, thereby allowing a simplified approach to the problem of joint probabilities of tides and surge.

Extreme sea levels around Prince Edward Island have been studied by CCAF (2001) and by Bernier & Thompson (2006, 2007). The Bernier work has been widely used as the basis for extreme water levels around PEI and is the basis for the surge levels used in Richards & Daigle (2011 and 2014). Storm surge patterns tend to linearly increase from north to

[§] http://www.isdm-gdsi.gc.ca

south with the largest surge amplitudes being observed along the south shore (Figure 3-11). The variation in surge magnitude is much smaller than the tidal variation. Expected surge magnitudes along the north shore are typically 90-95% of those along the south shore. Spatial variations in surge heights during storms are much more variable than these overall expected magnitudes. Depending on storm track and duration, storm surge can be localized to areas as small as a few tens of kilometres.

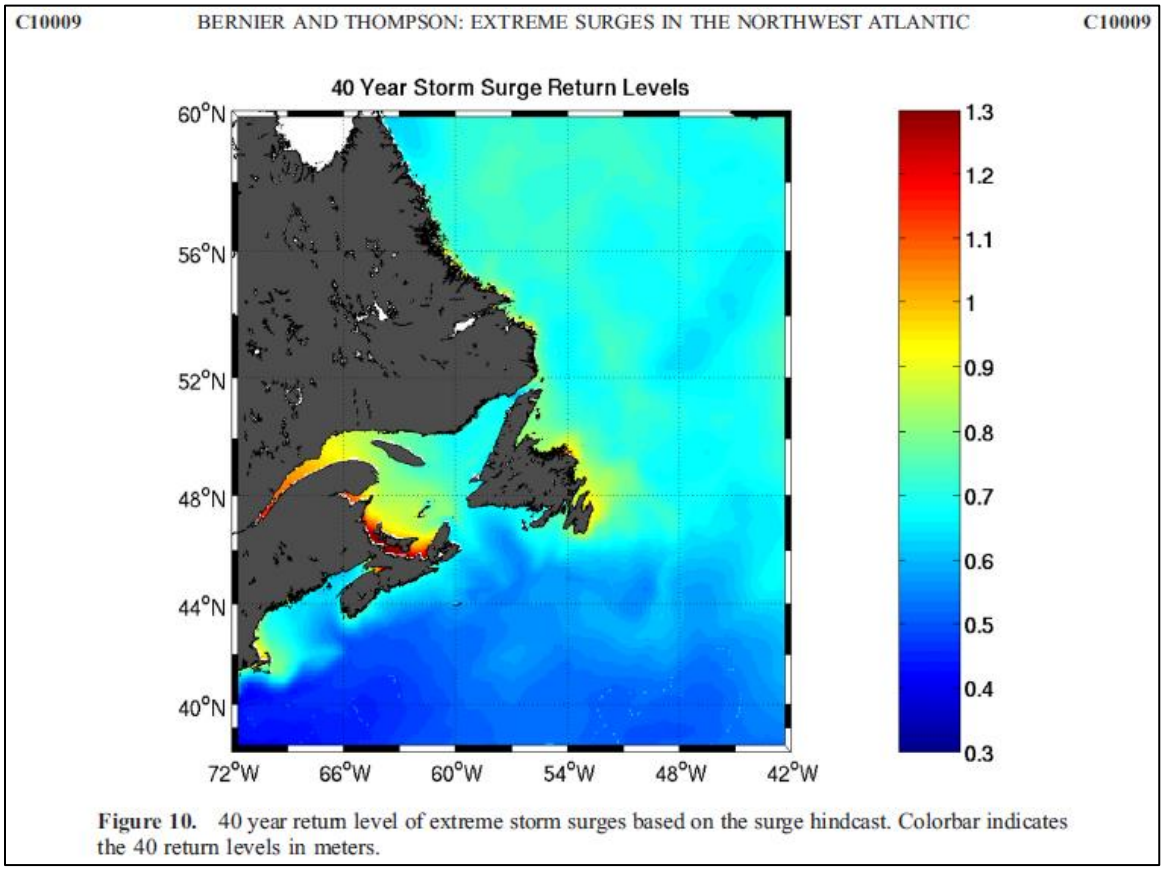

Figure 3-11 Map of storm surge elevations (Bernier and Thompson, 2006)

3.7 Joint Probalilites of Tide and Storm Surge

The joint probability of tides and storm surge is a relatively complex problem that varies around the Island. In Northumberland Strait, the incoming storm surge interacts with tidal currents leading to a blockage phenomenom which mean that storm surges in Northumberland Strait are almost twice as likely to occur at low tide than at high tide. Bernier & Thompson (2007) demonstrated this phenomenon using regional-scale circulation modelling (see Figure 3-12). This graph shows that large surges in Charlottetown are almost twice as likely to occur at low tide as they are at high tide.

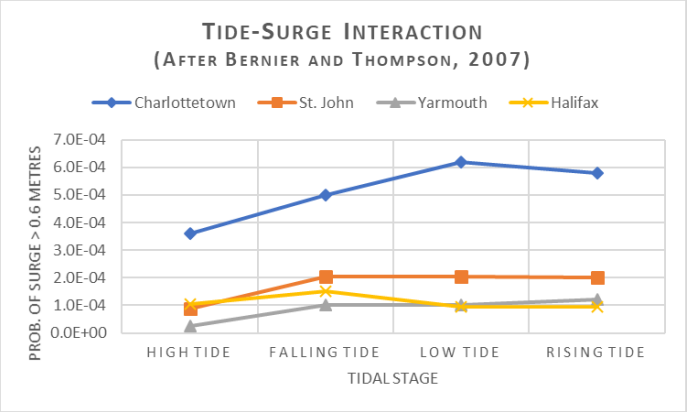

Figure 3-12 Tide-surge interaction at Charlottetown (from Bernier & Thompson, 2007)

Richards & Daigle (2011) recommended as a precautionary measure the use of HHWLT plus the 100-yr return period storm surge as estimated by Bernier (2006). An update to the Richards & Daigle flood scenarios (Daigle 2014) uses updated relative sea level rise numbers consistent with James et al (2014), but retains the same tide-surge relationships. Analysis presented in Section 5 of this report (and in Coldwater, 2018) has developed new extreme sea level predictions based on the expected joint probabilities of tides and surge.

3.8 Statistics of Extreme Values

In keeping with current practice, hazard likelihood is expressed herein by the Annual Exceedance Probability (AEP). AEP refers to the probability of a coastal flood hazard being met or exceeded in any given year, represented as a percentage. For example, an extreme coastal flood hazard that has a calculated probability of 1% of occurring in this or any given year is described as the 1% AEP coastal flood hazard. In the past, hazard likelihood was commonly represented as a 1 in n-year return period. However, this tends to give the false impression that a 100-year event is only expected to occur once every 100 years.

For example, a flood level of, say, 2 m above mean sea level, might have probability of being exceeded in any given year (AEP) of 1%. Such an event would have an annual (or yearly) exceedance probability, $P = 0.01$ and a return period, $T_R = 1/P = 100\ years$, suggesting that this level is expected to be exceeded, on average once in one hundred years.

The expected recurrence interval of a given storm condition is, however, not that simple. The encounter probability, or risk of exceedance of an event is a different, but related measure of extreme events. While an event might have a 1:100 (1%) chance of being exceeded in any given

year, the total chance of exceeding that level over a timespan of many years is much higher. The encounter probability, or risk, R is related to the annual probability of exceedance, $P(\eta)$, and the planning period, T_{PL} $(years)$ by the binomial distribution:

$$R = 1 - [1 - P(\eta)]^{T_{PL}}$$

The risk associated with, for example, the 1%AEP flood level is 0.01 in any given year, but over a planning horizon of, say 50 years, the chance of the flood level being reached is:

$$R = 1 - [1 - 0.01)]^{50} \; = \; 0.395$$

So, there is a 39.5% chance of water reaching the 1%AEP flood level within a 50-year planning horizon. A 100-yr planning horizon raises the risk to 63%, i.e. the odds are higher than 50:50 that the 1%AEP event will occur within 100 years (the 50:50 breakpoint in this case occurs at a planning time of 69 years). The relationship between return periods, timelines and risk is shown below in Table 3-2 and Figure 3-13.

Table 3-2 Risk and planning timeframes

	Planning timeframe, T_{PL} (years)				
AEP	10	25	50	75	100
100%	100%	100%	100%	100%	100%
20%	89%	100%	100%	100%	100%
10%	65%	93%	99%	100%	100%
4%	34%	64%	87%	95%	98%
2%	18%	40%	64%	78%	87%
1%	10%	22%	39%	53%	63%
0.40%	4%	10%	18%	26%	33%
0.10%	1%	2%	5%	7%	10%

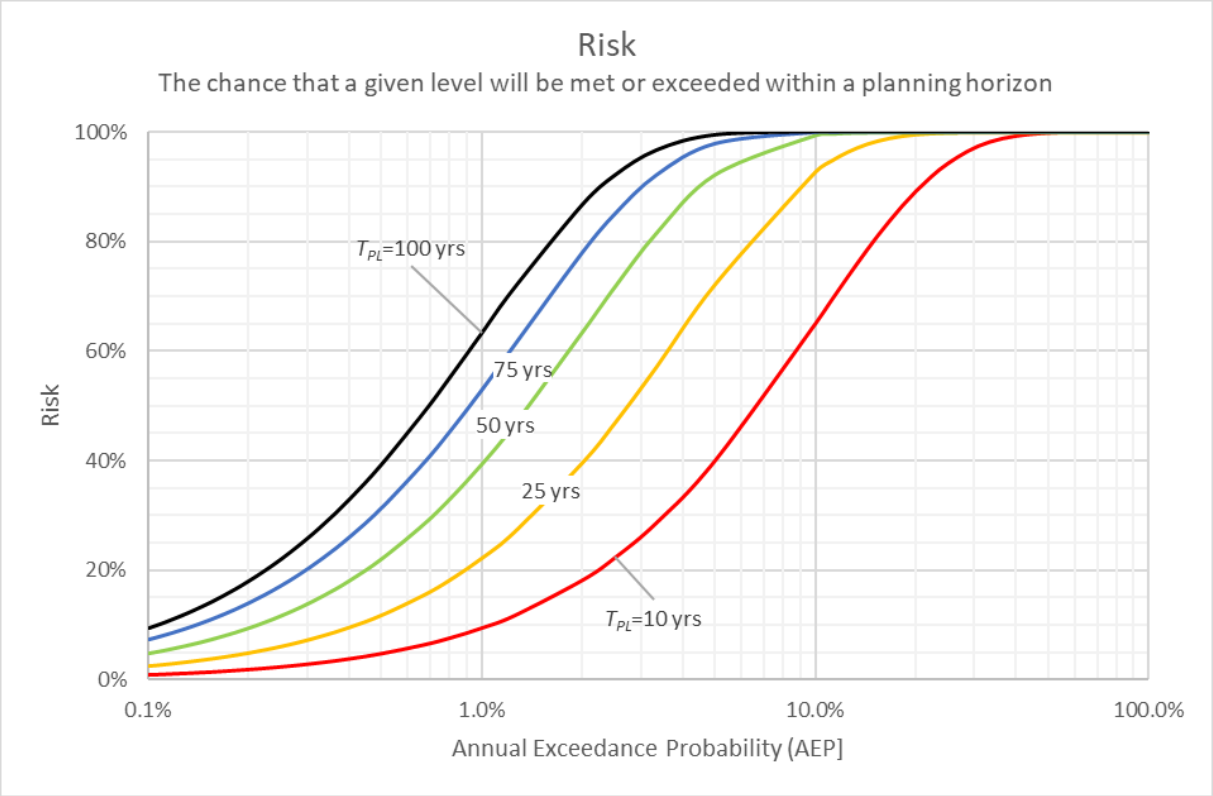

Figure 3-13 Risk as a function of AEP and planning timeframe

3.9 CAN-EWLAT

The Canadian Extreme Water Levels Adaptation Tool (CAN-EWLAT) has been developed by DFO to provide Canada-wide mapping of climate change related information for tide gauging stations and small craft harbour (SCH) sites. It provides:

- Relative sea level rise scenarios for each SCH site for given climate change scenarios,
- Vertical datum information (HyVSEP data),
- Vertical allowances to accommodate sea level rise (see below), and
- Maximum offshore significant wave heights winter/summer, current & projected.

This approach provides the advantages of:

- Comprehensive, consistent coverage for all Canadian sites,
- Vertical allowance analysis that is consistent with international efforts, and
- Wave climate forecasts that show forecast changes in storm intensity

The sea level allowance concept (Hunter 2012) allows assessment, on a regional scale, of the potential effects of sea level rise on coastal infrastructure. The sea level allowance is defined as the vertical distance that infrastructure assets would have to be raised under a given sea level rise scenario to maintain the same frequency of inundation as presently experienced. This is, essentially, a 'preservation of satisfaction' approach that allows the effects of sea level rise to be evaluated without *a priori* knowledge of site-specific structure elevations and characteristics. This approach does not include any consideration of wave conditions or local topography.

This sea level allowance approach has been applied by DFO (Zhai, Greenan, et al. 2013; Zhai, Greenan, et al. 2014) to 56 tide gauge stations along the coasts of Canada and in nearby US waters. Where tide gauge data is available, the technique uses empirical data on extreme sea levels obtained directly from tide gauge measurements, combined with estimates of relative sea level rise. The relative sea level rise estimates consider climate change effects, combined effects of local steric and dynamic sea level rise[**], and land subsidence/uplift associated with glacial isostatic adjustment (GIA). Projected regional sea level changes use the IPCC's AR5 RCP4.5 and RCP8.5 scenarios. Where no tide gauge data is available, extreme water level forecasts based on surge modelling are used to estimate extreme water level statistics (e.g. Bernier 2007). Figure 3-14 shows output from the CAN-EWLAT tool for Tracadie, PE.

The sea level allowance parameter, a_{CE} , as presented in Zhai et al (ibid) is computed from the statistics of the annual maximum water levels at a given site combined with the expected rise in relative sea level, Δz, and the associated standard deviation of the estimate of relative sea level rise, σ. This sea level allowance is defined as:

$$a_{CE} = \Delta z + \frac{\sigma^2}{2\lambda}$$

Here we use a_{CE} as the vertical sea level allowance to identify values of the sea level allowance retrieved directly from the DFO CAN-EWLAT site (termed, a in the DFO literature (Zhai, Greenan, et al. 2013)). This term includes the projected rise in relative sea level, Δz, as well as terms

[**] The term "steric" refers to the temperature, salinity, and pressure dependent specific volume of the ocean. "Dynamic" refers to changes in sea levels due to changes in the oceans' mass balance (meltwaters, hydrologic changes, etc.) and changes in oceanic and atmospheric circulation patterns.

relating to uncertainties in the sea level rise projections (σ^2), and the variability of extreme water levels at the site, λ.

This vertical allowance technique was originally developed by Hunter (2012). As detailed in Zhai et al (ibid), a Gumbel (GEV Type 1) probability distribution is used to compute a straight line of best fit of $z\ vs\ -ln(-ln(P))$. The slope of the resulting line (scale parameter, λ) and $z-$ intercept (location parameter, μ) are used to characterize the exposure of the site to extreme water levels. The $z-$intercept, μ is effectively the 1-year return period still water level. The scale parameter, λ reflects the variability of extreme water levels. A larger value of λ suggests a greater range in extreme water levels; structures in regions with higher λ values tend to be less sensitive to sea level rise. The ratio of σ^2 over λ capture the sensitivity of a site to variations in estimates of future sea level rise. This methodology was recently critically reviewed by Coldwater (Coldwater, 2018) for four DFO harbours around PEI (Naufrage, Skinner's Pond, Fishing Cove and Machon's Point) and was found to accurately capture the effects of relative sea level rise when compared to more detailed process-based joint probability analysis.

The CAN-EWLAT site provides access to HyVSEP values for 49 of PEI's DFO-SCH facilities. For example, at Tracadie in the year 2100 (Figure 3-14), CAN-EWLAT reports a vertical allowance of 0.92 m under the RCP8.5 climate scenario.

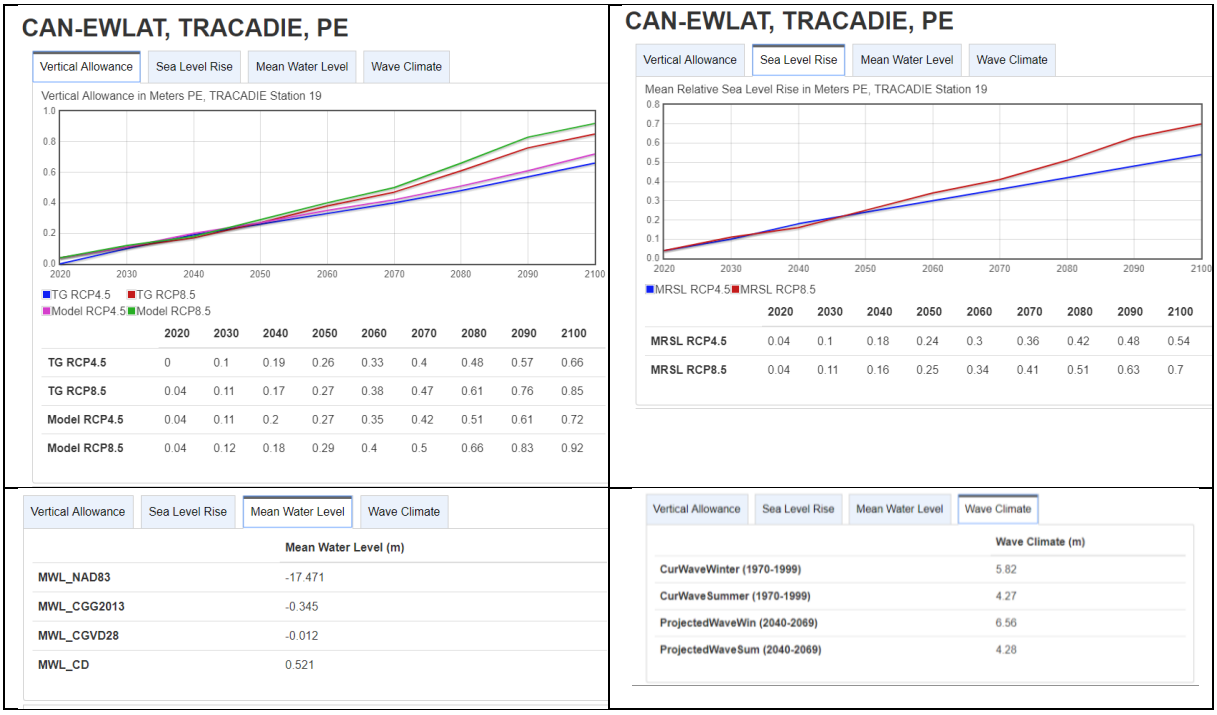

Figure 3-14 CAN-EWLAT output - Tracadie, PE

3.10 Charlottetown Water Levels

To illustrate the approach used for analysis of extreme water levels, the measured sea levels at Charlottetown have been de-trended by removing the linear trend in relative sea level rise between 1953 and 2015 and the annual maxima have been determined. Figure 3-15 shows the annual maxima by year of occurrence and Figure 3-16 shows the maxima sorted into rank-ascending order.

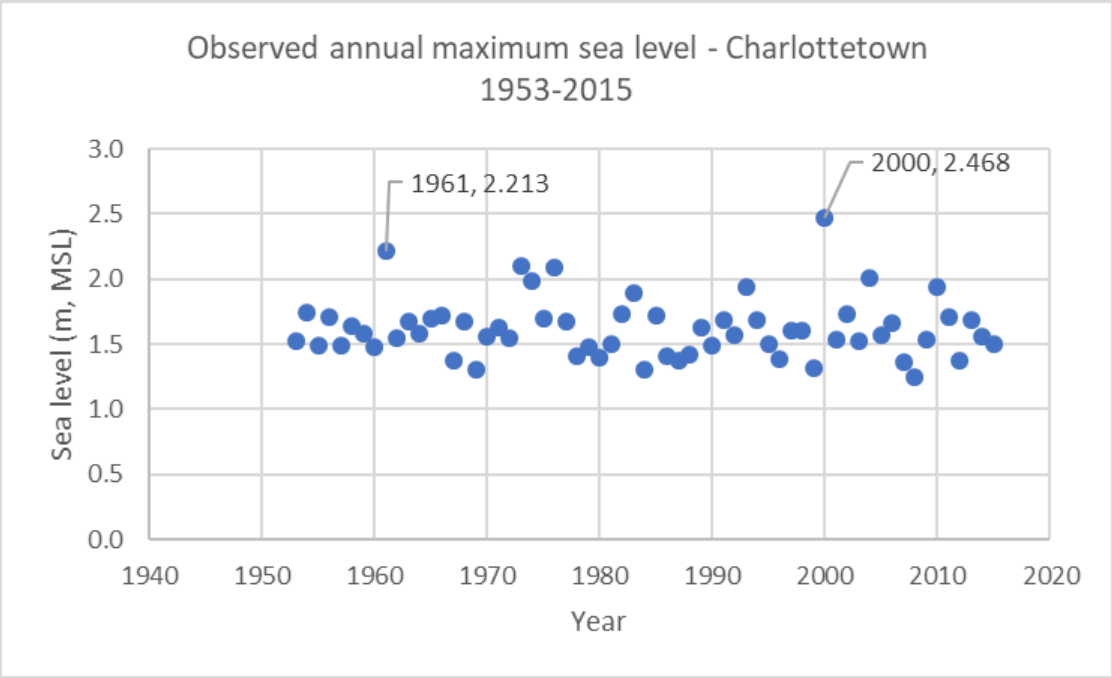

Figure 3-15 Annual maximum water levels at Charlottetown by year.

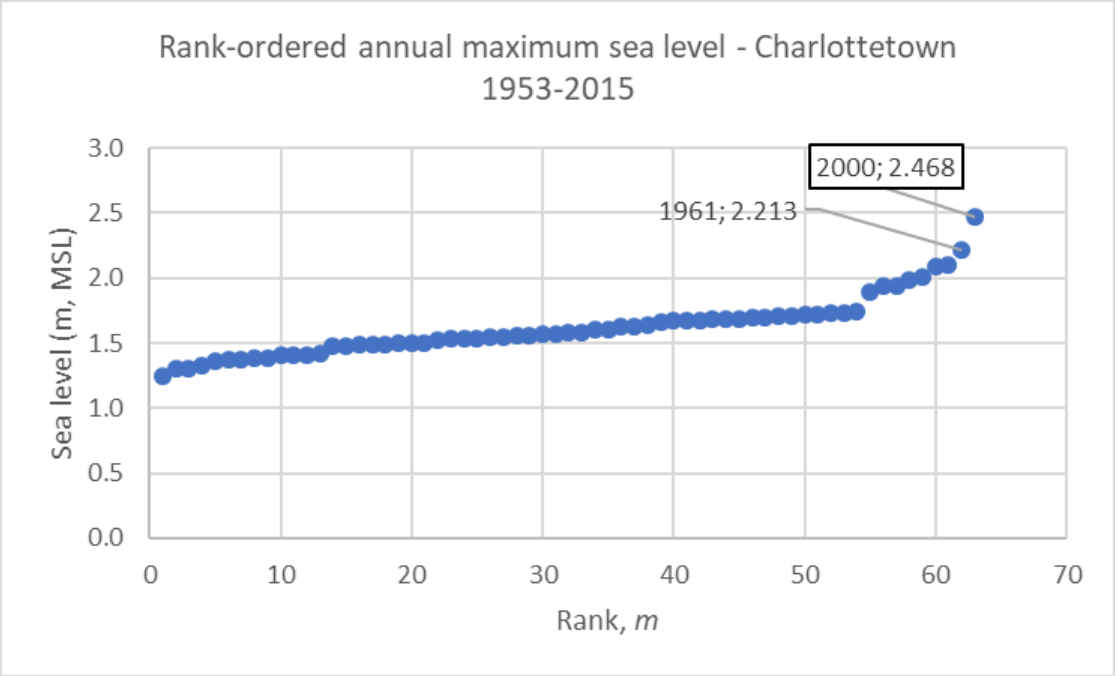

Figure 3-16 Rank-ordereed annual maximum water levels at Charlottetown.

The extreme values are then plotted against the Gumbel variate (T_R'):

$$T_R' = \frac{-1}{ln(1 - AEP)}$$

Figure 3-17 shows a plot of total water level, η, against T_R' and the straight-line of best fit (Type I GEV). The resulting relationship gives the extreme water level, η in term of a slope, λ and an offset, μ. In Zhai et al (ibid), λ and μ are referred to as the scale and location parameters, respectively.

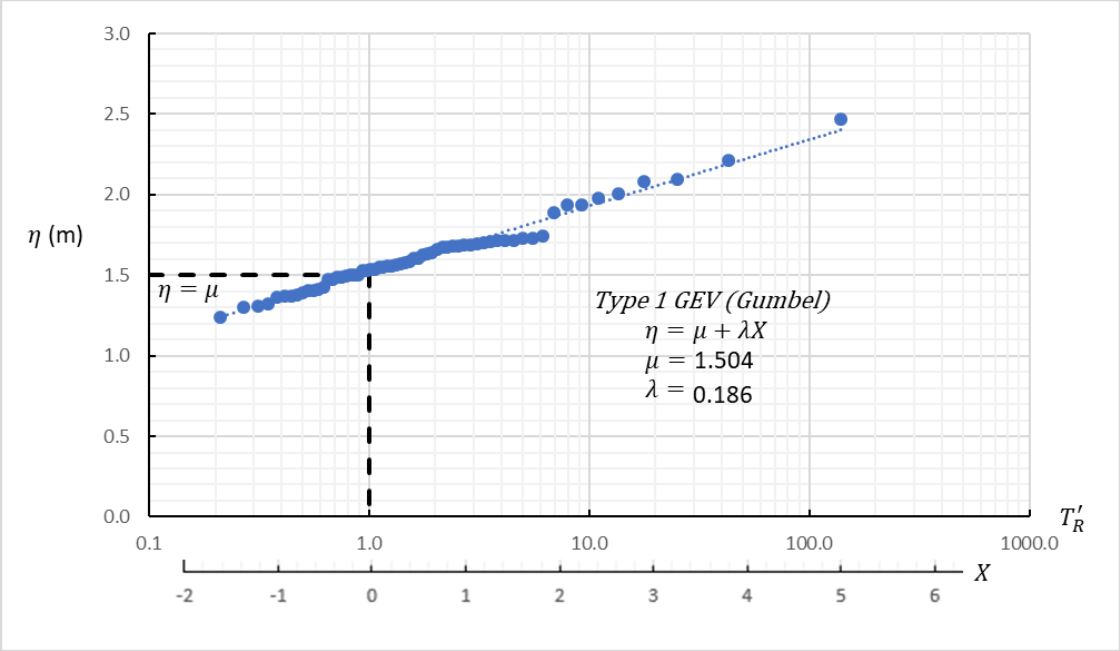

Figure 3-17 Extreme value analysis – Charlottetown total water levels

Alternatives to linear regression fitting of extreme value distributions include Maximum Likelihood (Coles, 2001) and the L-Moments method (Hosking, 1990). While generally more sophisticated and robust techniques, the resulting estimated extreme water levels using these techniques were seen to be within a few centimetres of those obtained by the simple log-linear regression technique. Opting for simplicity, the regression technique was employed for this study.

3.11 Surge Analysis

The Charlottetown hourly tide gauge data from 1953 through to 2015 was de-trended and cleaned to remove any irregularities (primarily due to gaps in the data record due to gauge maintenance and/or malfunction). Data gaps were filled with the predicted harmonic tide for that interval. This resulted in a water level time series that matches the duration of the MSC60 wave hindcast.

The total water level time series was then decomposed into a harmonic tidal signal and a residual surge signal. Under the assumption that large surge events affect the southern end of the Gulf of St. Lawrence is a somewhat uniform manner (and owing to a lack of other long-term gauge data), this surge signal was then used as a proxy for surge records for other sites around the island. The surge amplitude was scaled in accordance with the results of Bernier's (ibid) modelling and analysis and were time-shifted by up to 1 hour to account for surge propagation time around the Island based on the celerity of the M2 tidal wave. This

process resulted in a synthesized surge time series for each of the 13 tidal reference stations around the Island. Local harmonic tides were generated for each reference station using the DFO harmonic constituent database and then combined with the synthetic surge to give a continuous water level time series at each site.

The resulting total water level records were subjected to extreme value analysis to determine both tide and surge statistics at each site as well as the β-term described in Section 3.7.

While this method was both pragmatic and tractable, refinements clearly could be made in surge modelling around the Island. It is expected that opportunities will arise to refine the surge statistics as results from the new water level monitoring program (a separate part of this NDMP-funded initiative) become available.

3.12 Wave conditions

A wave hindcast uses a time series of known wind and wave conditions to predict the wave conditions at a given site. The analysis used herein is based on the MSC60 wave dataset (Swail, et al. 2006) which provides an hour-by-hour estimate of wave conditions throughout Maritime waters (the results are produced on a 0.1° grid across the Maritimes, including the Gulf of St. Lawrence and Northumberland Strait).

The MSC60 hindcast was used to establish offshore wave boundary conditions; the effects of wave shoaling and refraction (wave transformation) were addressed using the SWAN model (DUT 2009) as well as with Coldwater's in-house one-line wave transformation model. The SWAN runs were performed using both wind and wave boundary conditions and used a nested grid set up. The offshore grid was constructed with 100 m cells and extended to the MSC60 node used for the input wind and wave data. A set of high-resolution inshore grids with 2 to 10m spacing was used to model nearshore wave transformations, wave set-up and coastal inundation.

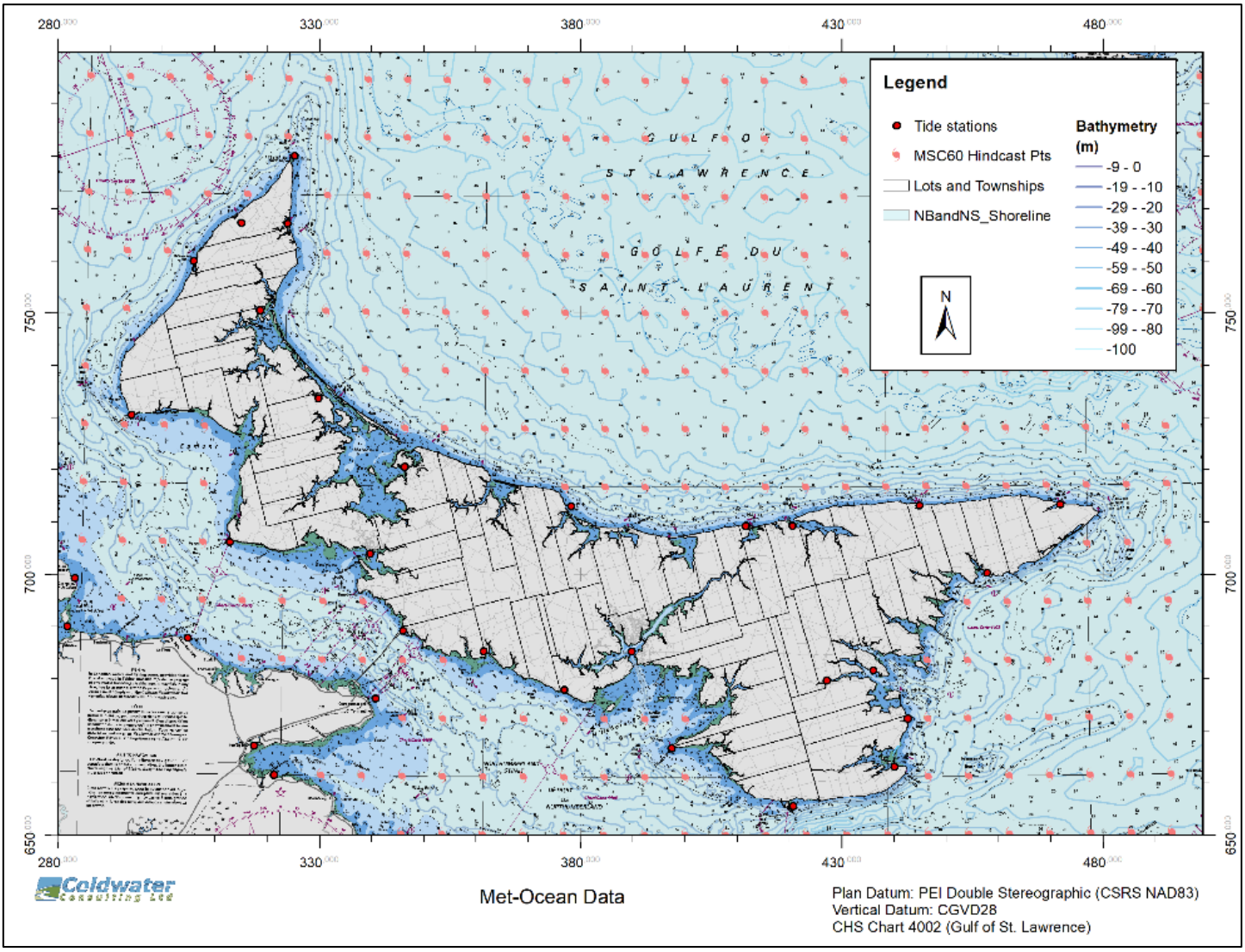

Figure 3-18 Dataset of nearest MSC50 nodes to the PEI shoreline

3.13 Wave Setup

Wave setup is the the increase in mean water level at the shore required to balance onshore gradients in wave momentum flux, typically associated with wave breaking. Wave setup is typically 3-10% of the offshore wave height (R. Dean, Wave Setup 2005), this can be an important component of nearshore water levels, allowing flood waters and wave action to reach further inland. Along PEI's north shore, significant wave heights of 5m would result in wave setup of 0.15 to 0.5m. Predictions of wave setup were extracted from the SWAN model and used to establish representative setup values to be used in the inundation mapping.

3.14 Coastal Overwash and Wave Runup

Wave action during storms can contribute to coastal flooding through wave coastal overwash in which low-lying plains are inundated by waves, wave setup and infra-gravity waves, and by wave runup on slopes.

Wave runup is one of the most technically challenging components of coastal flood hazard delineation. The vertical elevation reached by wave runup can be a critical factor in defining damage potential near the shore. Wave runup varies with wave height, H_s, wave period, T_p, and the slope over which the waves break (this can be the beach slope or the structure slope depending on the situation – or it can be a combination of the two slopes). Wave runup varies greatly with slope – a broad sandy beach will dissipate wave energy resulting in wave runup that is typically 4-7% of the incident wave height. For structures in relatively deep water, or those exposed to non-breaking waves, wave runup increases with slope steepness and can vary between 1.5 and 3 times the incident wave height.

Evaluating wave runup and overtopping can be the most technically challenging components of a coastal flood hazard assessment. The vertical elevation reached by wave runup can be a critical factor in defining damage potential near the shore. Wave runup varies with significant wave height, H_s, wave period, T_p, and the slope over which the waves break (this can be the beach slope or the structure slope depending on the situation – or it can be a combination of the two slopes). Wave runup is strongly influenced by the slope – a broad sandy beach will dissipate wave energy resulting in wave runup that is typically 4-7% of the incident wave height. For structures in relatively deep water, or those exposed to non-breaking waves, wave runup heights increase with slope steepness, and can be in the range 1.5 to 3 times the incident wave height.

For beaches, where wave energy is gradually dissipated through wave breaking, the vertical extent of wave runup, R_u is generally proportional to incident wave height, H_s and the surf similarity parameter, ξ_b.

$$\frac{R_u}{H_s} = \mathrm{f}(\xi_b)$$

$$\xi_{op} = \frac{m}{\sqrt{H_s / L_{op}}}$$

Here m is the cotangent slope, H_s is the significant wave height and L_o is the deepwater wavelength, $L_{op} = gT_p^2/(2\pi)$.

The surf similarity parameter provides a heuristic model for the surf zone, wave breaking, and for wave-structure interaction (Battjes and Janssen, Energy Loss and Set-up Due to Breaking of Random Waves 1978). The surf similarity parameter captures the width of the surf zone and the intensity of wave breaking. Battjes (1974) provided the following general guidance on interpreting ξ_{op}, noting that $1/\xi_{op}$ is approximately proportional to the number of wavelengths in the surf zone and that ξ_{op} is essentially proportional to the relative depth change across one wavelength in the surf zone. Table 3 is adapted from Battjes (1974) for the case of typical storm conditions with H_b/L_o=0.04. For typical sand/gravel beaches with slopes less than 0.01, (values of ξ_b less than 0.5) the surf zone is wide, and the wave breaking process is dissipative with spilling breakers, nearshore water levels are dominated by wave set-up and the actions of infra-gravity waves and surf-beat. As ξ_{op} increases (steeper beaches and/or lower wave steepness) the surf zone becomes narrower and less dissipative, wave breaking becomes more intense ranging from plunging to collapsing or surging. Under these conditions, the shore becomes more reflective and water levels become dominated by runup processes. These changes in beach behavior control runup: low ξ_{op} beaches are setup dominated while steeper shores, with collapsing/surging breakers, are runup dominated.

H/L_o=0.04						
m	0.002	0.01	0.1	0.2	0.5	1
ξ_{op}	0.01	0.05	0.5	1.0	2.5	5
N	10+	6-7	2-3	1-2	0-1	
	Breaking					No breaking
	spilling		plunging		collapsing/surging	clapotis/impulsive
H_s/d_b	0.6	0.8	1.0	1.1	1.2	
N	10+	6-7	2-3	1-2	0-1	
C_r	<0.1		0.1	0.15	0.4	0.6+
	absorption					reflection
	progressive wave					standing
	set-up dominated			run-up predominated		

H_s/d_b is the breaker index, N is the number of waves in the surf zone, C_r is the reflection coefficient

Table 3. Surf zone characterization for typical storm waves (H_b/L_o=0.04) adapted from Battjes & Jansen (1974).

Wave runup on individual structures requires a detailed and site-specific analysis. Parametric analysis using runup and overtopping predictors

such as those presented in EurOtop 2018 (van der Meer, Bruce, et al. 2018) are the most widely accepted methods. Newer techniques for 2-dimensional modelling of runup and overtopping are increasing in popularity and acceptance but remain time-consuming and highly specialized techniques that are used mostly in research and academic studies. Notable amongst recent developments is XBeach (Roelvink, et al. 2018) which was developed primarily as a a morphological model using the same hydrodynamic engine as SWASH (Smit, Zijlema and Stelling 2013). In recent years, the hydrodynamics of XBeach have been refined and extended to improve their applicability to problems of wave runup and overtopping. While earlier versions of XBeach used phase-averaged wave energetics, the model is now capable of phase-resolving wave modelling in depth-integrated or layered modes. The phase-averaged mode simulates infra-gravity wave action. XBeach has recently been successfully applied to reproduce the combined erosion and flooding processes generated by Hurricane Sandy (de Vet, et al. 2015). In Canadian waters, XBeach has recently been applied to the simulation of erosion and flooding processes at Maria, near the Gaspé (Didier, et al. 2019).

In the US, FEMA characterizes coastal flood hazards by a designated flood level (e.g. the 1%AEP storm tide elevation) and a wave envelope which describes the flood level including wave effects. In FEMA's terminology the elevation of the wave envelope is the BFE – the base flood elevation.

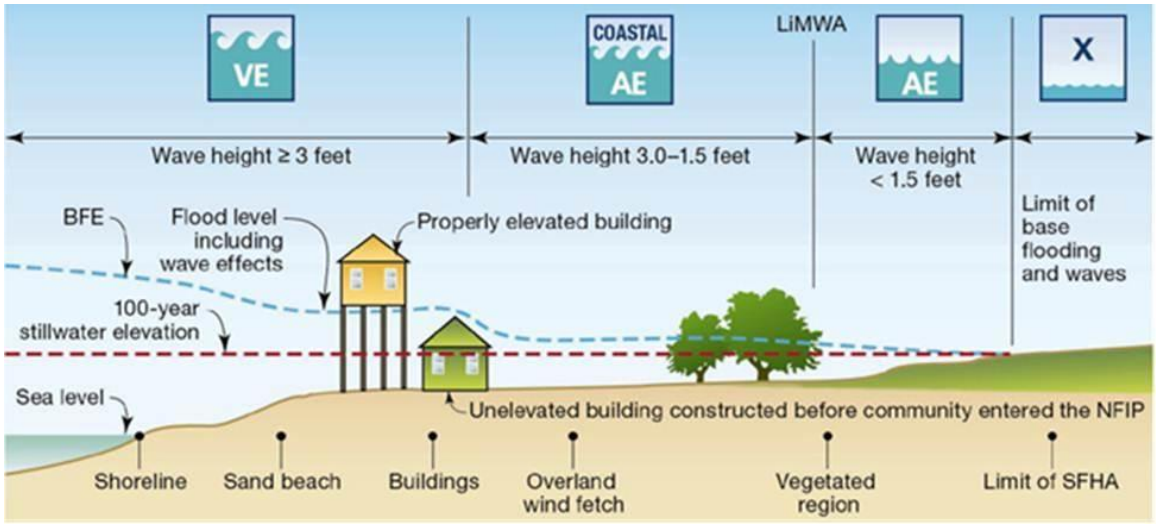

Figure 3-19 Flood hazard mapping used by FEMA (2018)

A similar approach has been adopted in BC (Kerrwood Leidal 2011) where a designated flood level (DFL) is defined based on relative sea level rise, tides, and storm surge. A Flood Construction Line (FCL) is defined as the recommended shoreward limit for any built

infrastructure, the FCL is mapped as an elevation contour, determined from an analysis of individual shore profiles. Setbacks from the FCL are then established on a lot-by-lot basis as the line where the FCL meets the original ground, but no less than 15m landward of the contour matching the DFL.

A major limitation of the FEMA and BC approaches is that they rely on a set risk level. For FEMA work (which forms the basis for national flood insurance mapping), the Designated Flood Level is based on the 1%AEP flood hazard. For BC it is based on the 0.5%AEP flood hazard.

In Canada, flood hazard delineation has typically been based on a fixed standards approach (Shrubsole, et al. 2003). Flood lines, for instance are typically based on one specific design flood (e.g. 1%AEP) for an entire region. By basing flood mapping on a single flood scenario, this approach fails to address the full range of possible flood scenarios, ranging from the cumulative effects of high frequency, low impact events to rare (exceptional) events which could have worse and farther-reaching impacts than the design flood. Similarly, it fails to adapt the standards to the vulnerability of the site or infrastructure in question. Standards-based approaches also lack the flexibility needed to address the dynamic nature of coastal flood risk in a changing climate.

International best practice is moving away from a fixed standards-based approach towards a risk-based approach (Sayers, et al. 2013). The idea is to no longer design solely for a single event focusing on safety and using engineered flood defences, but to use broader approaches that consider what is at risk and that maximizes social, economic and environmental benefits.

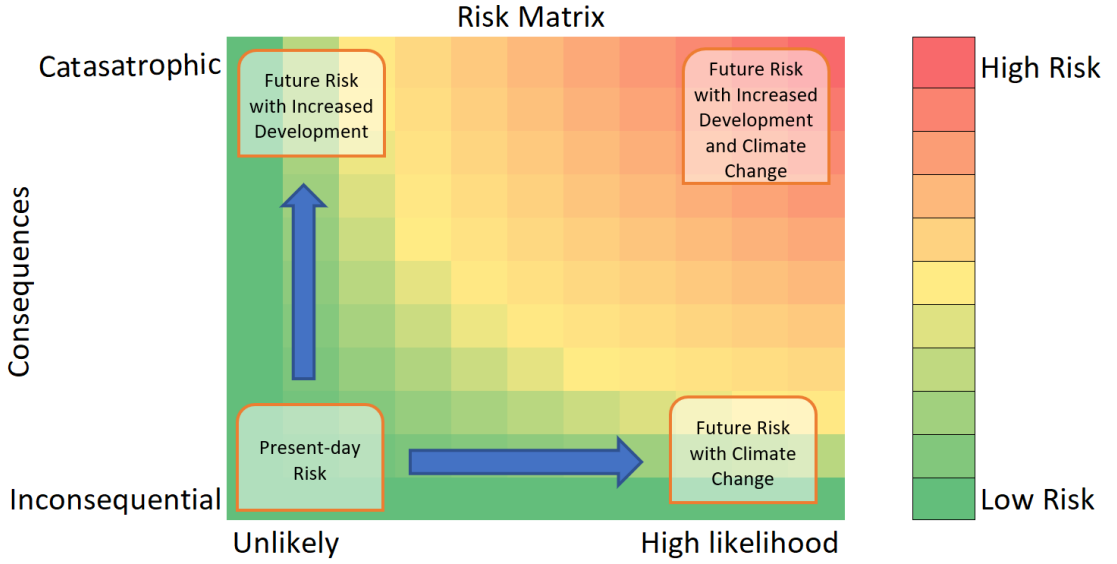

Figure 3-20 Risk Matrix (after Lyle, Wiebe, Davies et al, in press)

As a step toward developing a more flexible, risk-based approach to coastal flood hazards, the work presented herein has developed flood levels for a range of AEPs for present-day conditions, 2050 and 2100. The flood inundation maps have been produced only at the 1%AEP level (for present-day, 2050 and 2100) owing to the data storage implications of developing so many high-resolution maps as well as the cumbersome nature of having so many detailed maps.

The coastal flood hazard mapping prepared herein uses the wave envelope predicted from nearshore wave transformation modelling (SWAN) to derive base flood elevations in a manner similar to the FEMA approach.

Initial mapping was conducted with continuously spatially varying flood levels mapped onto the 2010 provincial shoreline. Upon review it was determined that this generated a data granularity that belied the fidelity of the input data. The mapping was subsequently revised to generate unique flood values for each of the 287 watersheds identified in the Provincial LiDAR-based watershed mapping ("PEI LIDAR WATERSHED BOUNDARIES 2008.shp").

4 Mapping Results

This section details for floodplain mapping process.

The Provincial 2008 LiDAR DEM dataset is arranged as a set of tiles (raster grids) in CSRS PEI Double Stereographic coordinates. There are a total of 256 tiles. The dataset has elevation data (CGVD28) on a 2m x 2m grid. This dataset is accompanied by a matching set of colour orthophotographs using the same tile footprints and numbering system. The DEM tiles have filenames DEM1 through DEM214 while the orthophotos are MAP1 through MAP214.

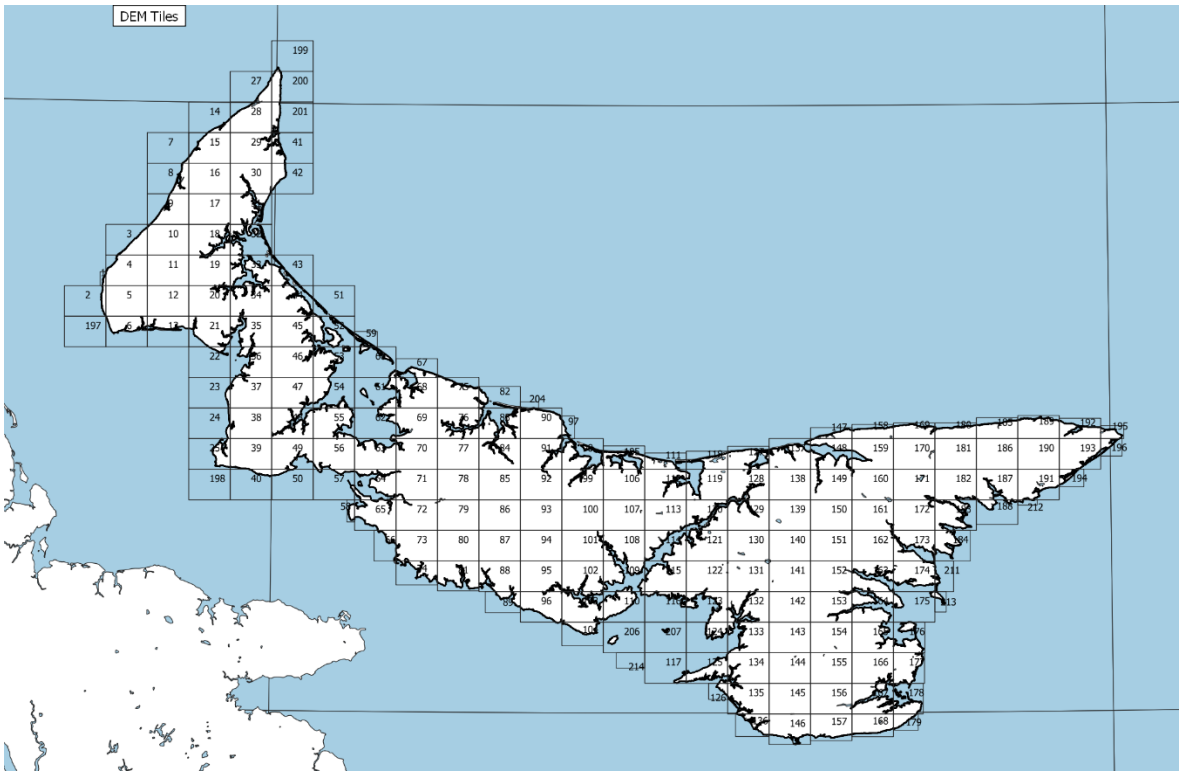

Figure 4-1 DEM and Ortho Tiles

4.1 Hydro-enforced DEMs

To create a hydro-enabled DEMs, the Provincial hydrology network (containing all watercourses) and the Provincial road network were loaded into the GIS. Culverts and or bridges were assumed to exist at each intersection of the road and stream networks. The University of Guelph's "Whitebox" toolset was used to cut into the DEM along the line of the stream. A maximum of 120m (60 pixels) was set to limit cut-in length while at the same time ensuring that the cut-in was sufficiently long to extend past the edges of the road embankments.

This resulted in a dataset of hydro-enforced DEMs (filenames DEM1_60 through DEM214_60 – indicating the use of a 60 pixel cut-in limit). This process was automated using python code running in the QGIS mapping software. Subsequent quality control inspection identified a handful of sites where the algorithm failed to properly cut the hydro-connection. These sites were edited by hand using on-screen DEM editing software within QGIS.

In Figure 4-2, the red diamonds indicate intersections between the road and stream networks where the DEM had to be modified to create a flow pathway.

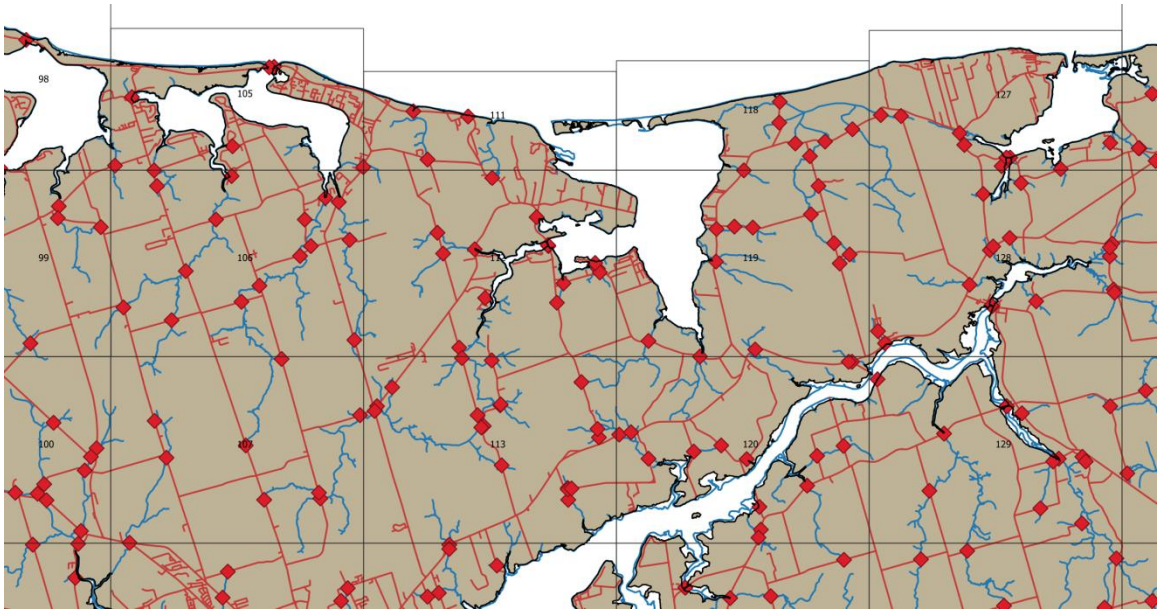

Figure 4-2 Stream network (blue), road network (red) and intersection points.

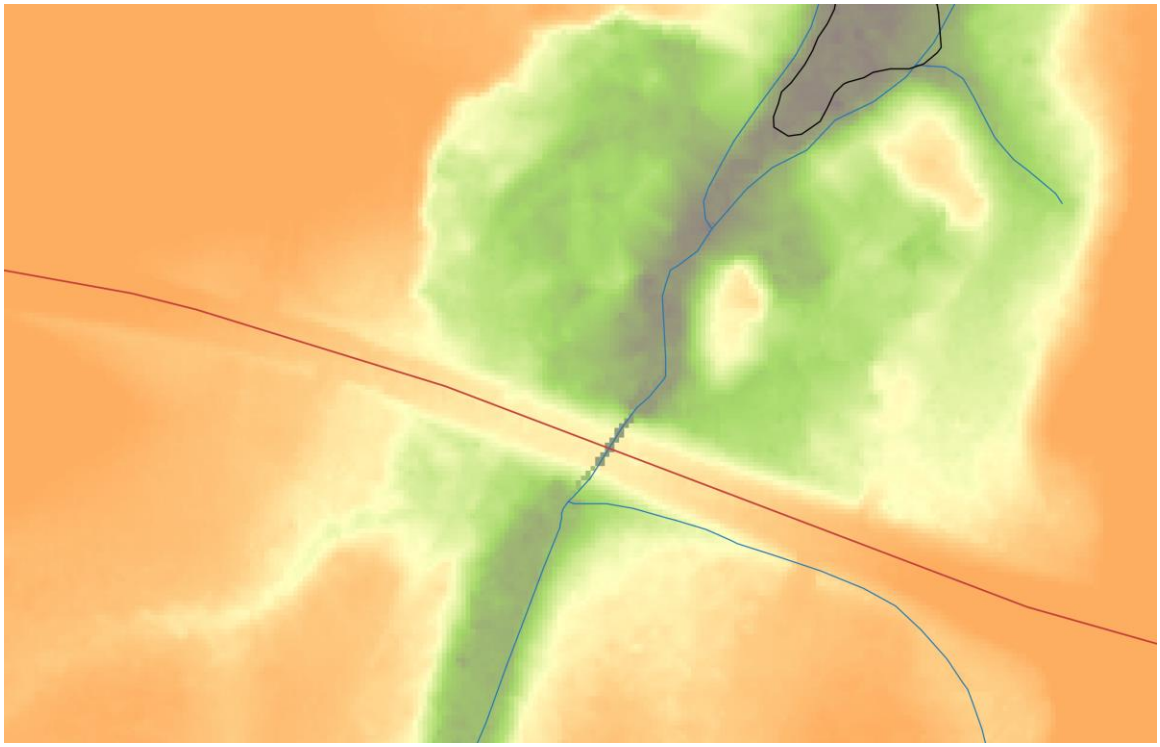

Figure 4-3 Steam crossing south of Savage Harbour showing cut-in of DEM to allow hydraulic connection through road embankment.

4.2 Wave Modelling

The SWAN model was setup to run on a set of nested cartesian (rectangular) grids. While an unstructured mesh (triangulated) would offer greater flexibility in model resolution and data handling, the computation of wave setup is only available when using cartesian grids.

Figure 4-4 shows the set of offshore wave grids used to transform waves from the nearest MSC60 grid nodes closer to shore. Figure 4-5 shows the set of 69 inshore grids that were used to model the nearshore at much higher resolution (between 2 and 10m grid spacing. Results from the offshore grids were used to derive boundary conditions for the inshore grids.

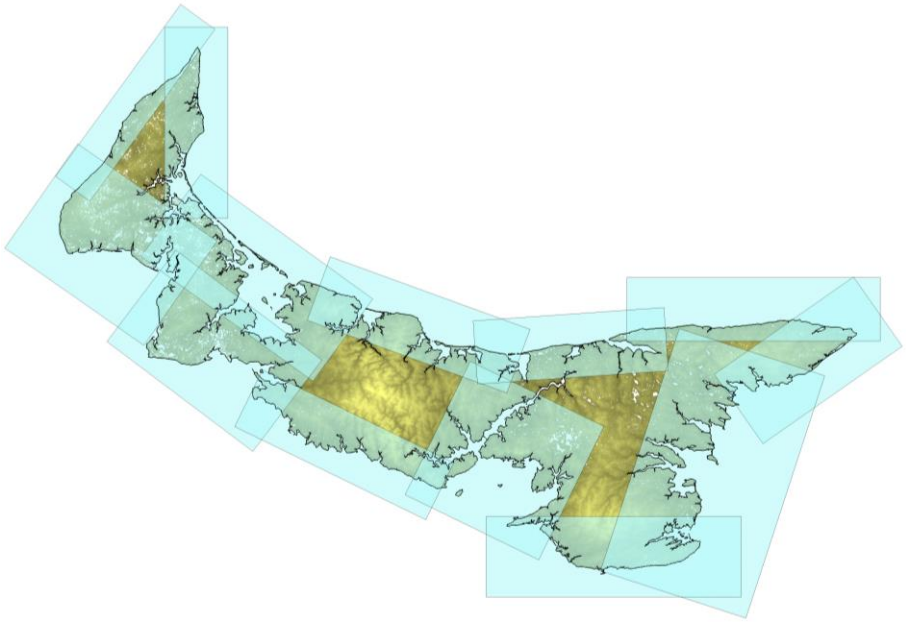

Figure 4-4 Offshore SWAN grids

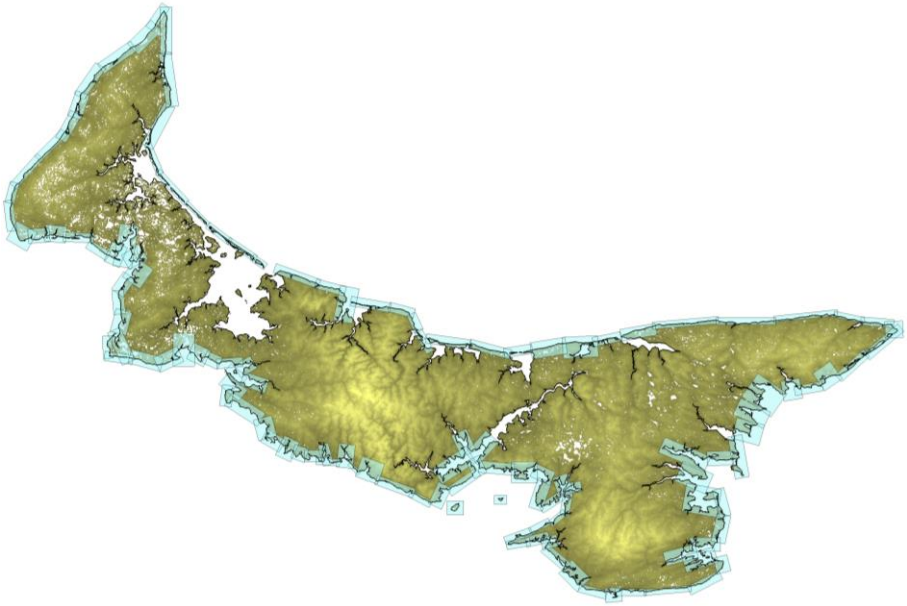

Figure 4-5 Inshore SWAN grids

Figure 4-6 shows the set of 16 estuary grids that were used to model wave conditions in major estuaries at high resolution (between 2 and 10m grid spacing).

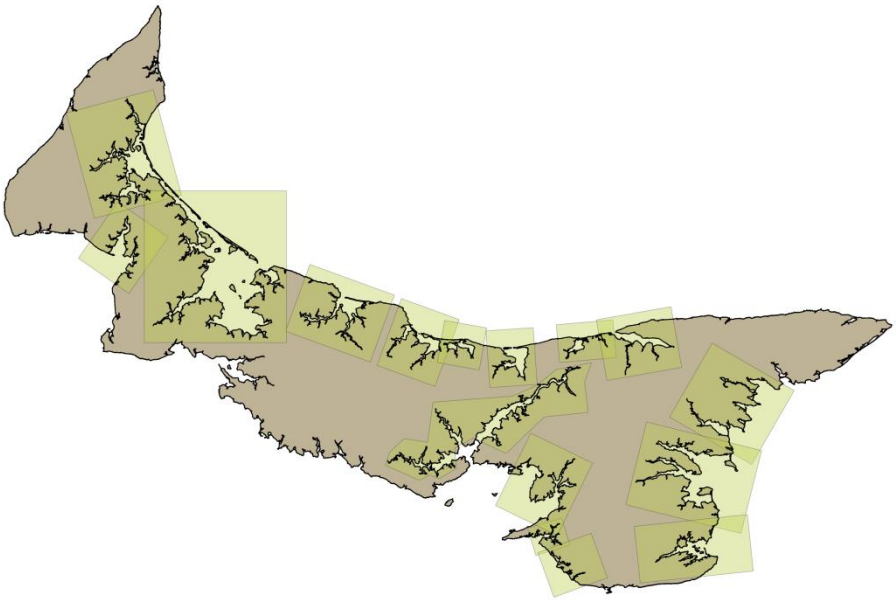

Figure 4-6 Estuary SWAN grids

A typical wave setup result is shown in Figure 4-7, which shows the computed wave setup at Savage Harbour.

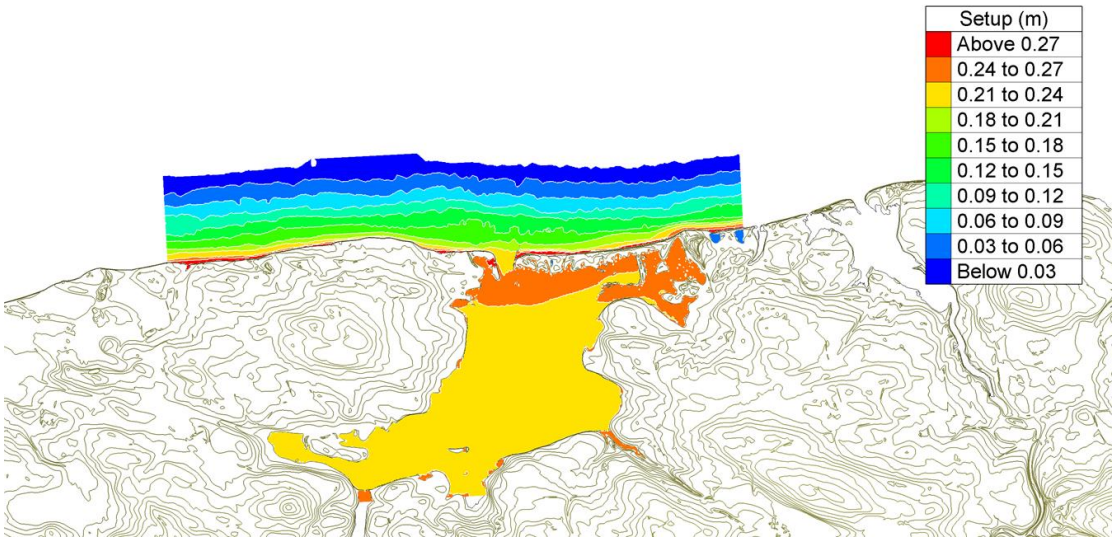

Figure 4-7 SWAN results (wave setup) on inshore grid at Savage Harbour

Preliminary analysis of nearshore wave conditions showed depth-limited waves under most situations. Wave modeling focussed on the 1%AEP wave event. Wave data was processed to obtain H_s, and setup for the 1%AEP wave event at present-day and year 2100 levels. The 1%AEP onshore-directed wave conditions were determined by statistical analysis of all MSC60 offshore wave grids around the Island. In sheltered waters (such as inside estuaries), locally-generated waves were synthesized using a parametric hindcast based on a site-specific fetch analysis and offshore winds from the MSC60 dataset. In modelling the 1%AEP storm conditions, multiple wave directions and wave periods

were considered, and the worst-case scenario was carried forward for the coastal hazard analysis.

Maps of nearshore wave heights and wave setup were extracted from the SWAN dataset and converted into geotiff raster data files for use within the GIS.

Base Flood Elevation (BFE) maps were generated from the SWAN results using the wave setup and the peak wave envelope height, $\hat{\eta}$. These were also exported as ascii point files (.csv format) for use in the GIS.

A supplemental set of Base Flood Depth (BFD) maps were generated that present the flood surfaces in terms of the local water depth during the event. These can also readily be derived within the GIS software by subtracting the DEM topography (land elevations) from the BFE surfaces.

The SWAN modelling, due to its computational intensity, was limited to coastal and estuarine waters. To extend flood inundation inland to cover all streams and channels, a GIS-based flooding algorithm was used over the hydro-enforced DEM. The resulting inundation mapping was generated as a series of tiff format raster tiles that match the DEM tile coverage. Tiles representing the 1%AEP flood scenario under present-day and year 2100 conditions were generated.

The establishment of flood plain mapping at a 2mx2m scale including wave effects is, in a sense, a double-edged sword. The detail and resolution provide exceptional accuracy and utility, but at the same time create logistical challenges with manipulating and presenting such a quantity of data. Attempts to map the results of the floodplain mapping back to simpler data structures such as the 2010 vector shoreline failed to generate a useful and reliable indicator of flood hazard.

Upon review it was determined that watershed-based mapping of flood levels would capture the spatial variations in flood levels and allow presentation of the data in coherent blocks with consistent results within each watershed.

5 Closing

This report has described coastal hazard analysis conducted for the Province of PEI.

The material contained herein reflects the judgement of Coldwater Consulting Ltd. in light of the information available to them at the time of preparation. Any use which a Third Party makes of this report, or any reliance on decisions to be made based on it, is the responsibility of such Third Parties. Coldwater Consulting Ltd. accepts no responsibility for damages, if any, suffered by any Third Party as a result of decisions made or actions based on this report.

This report was prepared by M. Davies of Coldwater Consulting Ltd., for further information please contact:

mdavies@coldwater-consulting.com
Mike Davies, Ph.D. ,P .Eng.
Coldwater Consulting Ltd.

6 Bibliography

Ausenco Sandwell. 2011. "Guidelines for Management of Coastal Flood Hazard Land Use." Report to BC Ministry of Environment, 27 Jan 2011.

Battjes, J.A. 1974. "Surf Similarity." *14th International Conf. Coastal Engg.* Copenhagen: ASCE. 466-480.

Battjes, J.A., and J. Janssen. 1978. "Energy Loss and Set-up Due to Breaking of Random Waves." *International Conference on Coastal Engineering.* Hamburg: ASCE. 569-587.

BC Environment. 2012. *Flood hazard area land use management guidelines.* On-line documentation, Victoria: eng.gov.gc.ca/wsd/public_safety/flood/fhm-2012/.

Bernier, N.B., and K.R. Thompson. 2006. "Predicting the frequency of storm surges and extreme sea levels in the northwest Atlantic." *J. Geophysical Research* C1009.

Bernier, N.B., and K.R. Thompson. 2007. "Tide-surge interaction off the east coast of Canada and northeastern United States." *J. Geophysical Research, Vol. 112* C06008.

Bernier, N.B., Thompson, K.R., Ou, J., Ritchie, H. 2007. "Mapping the return periods of extreme sea levels: Alllowing for short sea level records, seasonality, and climate change." *Globa and Planetary Change* (Elesvier) 57: 139-150.

CCAF A041 Project Team. 2001. *Coastal impacts of climate change and sea-level rise on Prince Edward Island.* Dartmouth, Nova Scotia: Climate Change Actoin Fund project CCAF A041, 74.

CIRIA. 2007. "The Rock Manual - The use of rock in hydraulic engineering (2nd ed)." C683, London.

Daigle, R. 2014. *Updated Sea-Level Rise and Flooding Estimates for New Brunswick Coastal Sections.* Moncton, NB: R.J. Dible Enviro.

Davidson-Arnott, R. 2005. "Conceptual Model of the Effects of Sea Level Rise on Sandy Coasts." *Journal of Coastal Research* 24 (6): 1166-1172.

Davies, M.H. 2012. *Geomorphic Classification of Prince Edward Island.* Atlantic Climate Adaptation Solutions, 85.

Davies, M.H. 2011. *Shore Protection and Climate Change.* Charlottetown, PE: Atlantic Climate Adaptation Solutions Association. Accessed 04 17, 2016.

Davies, M.H., and N.J. MacDonald. 2016. *Charlottetown Watefront Coastal Vulnerability Assessment.* Charlottetown: Report prepared for Charlottetown Area Development Corporation.

Davies, M.H., and N.J. MacDonald. 2018. *Climate Change, Coastal Hazards and Vulnerability - PEI Harbours.* Report prepared under contract to FIsheries & Oceans Canada, Small Craft Harbours Directorate, Ottawa, Coldwater Consulting Ltd.

Davies, M.H., and N.J. MacDonald. 2016. *Coastal Engineering Assessment Impacts of Climate Change and Sea Level Rise Mi'kmaq Communtities of Prince Edward Island.* Report prepared for Mikmaq Communities of PEI (MCPEI), Ottawa: Coldwater Consulting Ltd.

Davies, M.H., and N.J. MacDonald. 2016. *Coastal Engineering Assessment of the Impacts of Climate Change and Sea Level Rise on the Mi'kmaq Communities of the Bras d'Or Lakes.* Report prepared for the Unama'ki Institute of Natural Resources, Ottawa: Coldwater Consulting Ltd.

de Vet, P.L.M., R.T. McCall, J.P. den Bieman, Marcel J.F. Stive, and M. van Ormondt. 2015. "Modelling Dune Erosion, Overwash And Breaching At Fire Island (Ny) During Hurricane Sandy." *Proc. Coastal Sediments 2015.* San Diego, US: World Scientific. https://doi.org/10.1142/9789814689977_0006.

Dean, R.G. 1991. "Equilibrium Beach Profiles: Characteristics and Applications." *J. Coastal Research* Vol 7 (1).

Dean, R.G. 2005. *Wave Setup .* FEMA Coastal Flood Hazard Analysis and Mapping Guidelines, Focussed Study Report.

Dean, R.G., and J.R. Houston. 2016. "Determining shoreline response to sea level rise." *Coastal Engineering* 114 1-8.

Dean, R.J., I. Collins, D. Divoky, D. Hatheway, and N. Scheffner. 2005. *Wave Setup.* Coastal Flood Hazard Analysis and Mapping Guidelines; Focussed Study Report, FEMA.

DELWP. 2017. *Guidelines for developing a coastal hazard assessment.* Victoria State Government.

Di Luccio, D., G. Benassai, G.. Budillon, L. Mucerino, R. Montella, and E.P. Carratelli. 2018. "Wave run-up prediction and observation in a micro-tidal beach." *Nat. Hazards Earth Syst. Sci.* 18 2841-2857.

Didier, D., M. Bandet, P. Bernatchez, and D. Dumont. 2019. "Modelling coastal flood propagation under sea level rise: A case study in Maria, Eastern Canada." *Geosciences* 9.76.

Douglass, S., and J. Krolak. 2008. *Highways in the Coastal Environment, HEC 25, Vol. 1, 2nd ed.* FHWA NHI-07-096, Washington, DC: US Federal Highways Administration.

Douglass, S., B. Webb, and R. Kilgore. 2014. *Highway in the Coastal Environment: Assessing Extreme Events, HEC No. 25 Vol. 2.* FHWA-NIH-14-006, Washington, DC: US Federal Highways Administration.

Duncan, M.F., M.S. Fenster, B.A. Argow, and I.V. Buynevish. 2008. "Effects of sea level rise on barrier islands IN Coastal Impacts Due to Sea-Level Rise." *Ann. Revue Earth Planetary Sciences* 36:601-647.

DUT. 2009. *SWAN User Manual.* Delft, NL: The SWAN Team, Delft University of Technology.

FEMA. 2018. *Coastal Floodplain Mapping.* Guidance for Flood Risk Analysis and Mapping, Washington, DC: US Federal Emergency Management Administration.

FEMA. 2018. *Coastal Wave Runup and Overtopping.* Guidance Document 89, Washington, DC: U.S. Federal Emergency Management Agency.

FEMA. 2007. *Guidelines and Specifications for Flood Hazard Mapping Partners* . Section D.2.8, Washington, DC: U.S. Federal Emergency Management Administration.

Forbes, D.L., Parkes, G.S., Manson, G.K. and Ketch, L.A. 2004. "Storms and shoreline retreat in the southern Gulf of St. Lawrence." *Marine Geology (210)* (Elsevier) 210: 169-204.

Fraser, C., P. Bernatchez, and S. Dugas. 2017. "Development of a GIS coastal land-use planning tool for coastal erosion adaptation based on the exposure of buildings and infrastructure to coastal erosion, Quebec, Canada." *Geomatics, Natural Hazards and Risk* 8:2 1103-1125.

Goda, Y. 2011. "Plotting position estimator for the L-moment method and quantile confidence interval for the GEV, GPA, AND Weibull distributions applied for extreme wave analysis." *J. Coastal Engg.* 53 (2): 111-149.

Gornitz, V., T.W. White, and R.W. Cushman. 1991. "Vulnerability of the US to future sea-level rise." *7th Symposium on Coastal and Ocean Management.* Long Beach, CA: ASCE. 2354-2368.

Gringorten, I.I. 1963. "A plotting rule for extreme probability paper." *J. Geophys. Res. 68* 813-814.

Han, G., Z. Ma, L. Zhai, B. Greenan, and R. Thomson. 2016. *Twenty-first century mean sea level rise scenarios for Canada.* Canadian Technical Report of Hydrography and Ocean Sciences 313, Fisheries and Oceans Caanada.

Hazen, A. 1914. "Storage to be provided in impounding reservoirs for municipal water supply." *Trans. Americ. Soc. Civ. Eng. Pap. 1308 (77)* 1547-1550.

Hegde, A.V., and V.R. Reju. 2007. "Development of a Coastal Vulnerability Index for Mangalore Coast, India." *J. Coastal Research* 1106-1111.

Hosking, J.R., and J.R. Wallis. 1995. "A comparison of unbiased and plotting-position estimators of L-moments." *Water Res. 31* 2019-2025.

Houston, J.R., and R.G. Dean. 2014. "Shoreline change on the East coast of Florida." *J. Coastal Research* V30(4) 647-660.

Hunter, J. 2012. "A simple technique for estimating an allowance for uncertain sea-level rise." *Climatic Change* Vol. 113 No. 2 pp. 239-252.

IHO. 2011. *Manual on Hydrography, IHO Publication C-13.* Monaco: International Hydrographic Organization, 480.

J. Hansen, M. Sato, P. Hearty, R. Ruedy, M. Kelley, V. Masson-Delmotte, G. Russell, G. Tselioudis, J. Cao, E. Rignot, I. Velicogna, E. Kandiano, K. von Schuckmann, P. Kharecha, A. N. Legrande , M. Bauer, and K.-W. Lo. 2015. "Ice melt, sea level rise and superstorms: evidence from paleoclimate data, climate modeling, and modern observations that 2◦C global warming is highly dangerous." *Atmospheric Chemistry and Physics (ACP)* (20059–

20179) 15 (15): 20059–20179. Accessed 12 8, 2016. http://www.atmos-chem-phys-discuss.net/15/20059/2015/acpd-15-20059-2015.pdf.

James, T.S., J.A. Henton, L.J. Leonard, A. Darlington, D.L. Forbes, and M. Craymer. 2014. *Relative Sea-level Projections in Canada and the Adjacent Mainland United States.* Geological Survey of Canada, Open File 7737, 72 p. doi:10.4095/295574.

James, T.S., J.A. Henton, L.J. Leonard, A. Darlington, D.L. Forbes, and M. Craymer. 2014. *Relative Sea-level Projections in Canada and the Adjacent Mainland United States.* Geological Survey of Canada, Open File 7737, 72 p. doi:10.4095/295574. http://geoscan.nrcan.gc.ca.

James, T.S., J.A. Henton, L.J. Leonard, A. Darlington, D.L. Forbes, and M. Craymer. 2014. *Relative Sea-level Projections in Canada and the Adjacent Mainland United States.* Geological Survey of Canada, Open File 7737. http://geoscan.nrcan.gc.ca.

Jevrejeva, S., A. Grinsted, and J.C. Moore. 2014. "Upper limit for sea level projections by 2100." *Environ. Res. Lett.* (9) 104008 9 pp. doi:doi:10.1088/1748-9326/9/10/104008.

Johnson, B.D., N. Kobayashi, and M.B. Gravens. 2012. *Cross-shore numerical model CSHORE for waves, currents, sediment transport and profile evolution.* TR-12-22, Vicksburg, MS: USACE-ERDC-CHL.

Kerrwood Leidal. 2011. *Coastal Floodplain Mapping - Guidelines and Specifications.* Final report to BC Ministry of Forests, Lands and Natural Resource Operations, 91.

Lemmen, D.S., F.J. Warren, T.S. James, and C.S.L. Mercer-Clarke. 2016. *Canada's Marine Coasts in a Changing Climate.* Ottawa: Government of Canada, 274.

Li, H., L. Lin, and K.A. Burks-Copes. 2012. "Numerical modelling of coastal inundation and sedimentation by storm surge, tides and waves at Norfolk, VA." *Proc. 33rd Int'l Conf on Coastal Engg .* 14.

Makkonen, L. 2005. "Plotting positions in extreme value analysis." *J. Applied Meteorology and Climatology, AMS* 45: 334-340.

Mase, H., T. Tamada, T. Yasuda, T. Hedges, and M. Reis. 2013. "Wave runup and overtopping at seawalls built on land and in very shallow water." *J. Waterway, Port, Coastal and Ocean Engg. (ASCE)* 346-357.

Melby, J.A. 2012. *Wave runup prediction for flood hazard assessment.* TR-12-24, Vicksburg, MS: USACE-ERDC-CHL.

Melby, J.A., N.C. Nada-Caraballo, and N. Kobayashi. 2012. "Wave runup prediction for flood mapping." *Coastal Engineering.* ASCE.

Murphy, E., T. Lyle, J. Wiebe, S.V. Hund, M. Davies, and D. Williamson. 2020. *Coastal Flood Risk Assessment Guidelines for Building and Infrastructure Design.* ISBN 978-00-660-36745-3, Ottawa: National Research Council of Canada.

Natural Resources Canada. 2018. *Federal Flood Mapping Framework.* General Information Product 112e, (V2.0), Ottawa: Gov. of Canada.

Natural Resources Canada. 2019. *Federal Hydrologic and Hydraulic Procedures for Flood Hazard Delineation.* General Information Product 113e (V1.0), Ottawa: Gov. of Canada.

Nicholls, R.J., and R.J. Klein. 2005. *Climate change and coastal management on Europe's coast.* Germany, Springer: in Vermaat, J., Bouwer, L., Turner, K. and Salomons, W. (eds) 2005 Managing Europe's Coasts: Past, Present and Future.

Pethick, John S., and S. Crooks. 2000. "Development of a Coastal Vulnerability Index: a Geomorphological Perspective." *Environmental Conservation* 27 (4): 359–67.

Poate, T.G., R.T. McCall, and G. Masselink. 2016. "A new parameterization for runup on gravel beaches." *Coastal Engg. 117* 176-190.

Pugh, D.T. 1987. *Tides, Surges and Mean Sea-Level.* Wiltshire, UK: John Wiley & Sons Ltd.

Pullen, T., N.W.H Allsop, T. Bruce, A. Kortenhaud, H. Schuttrumpf, and J.W. van der Meer. 2007. *EurOtop - Wave Overtopping of Sea Defences and Related Structures: Assessment Manual.* www.overtopping-manual.com .

Ramieri, E., A. Hartley, A. Barbanti, F.D. Santos, A. Gomes, M. Hilden, P. Laihonen, N. Marinova, and M. Santini. 2011. *Methods for assessing coastal vulnerability to climate changes.* Thetis (Italy): The European Topic Centre on Climate Change Impacts, European Environment Agency (ETC CCA).

Ranasinghe, R., D. Callaghan, and M.F. Stive. 2012. "Estimating coastal recession due to sea level rise: beyond the Bruun rule." *Climatic Change* V110 No 3-4, pp 561-574.

Richards, W., and R. Daigle. 2011. *Scenarios and Guidance for Adaptation to Climate Change and Sea-Level Rise - NS and PEI Municipalities.* Dartmouth, NS: Atlantic Canada Adaptations.

Robin, C., S. Nudds, P. Macaulay, A. Godin, B. de Lange Boom, and J. Bartlett. 2016. "Hydrographic Vertical Separation Surfaces (HyVSEPs) for the Tidal Waters of Canada." *Marine Geodesy* (39) 195-222.

Roelvink, D., R. McCall, S. Mehvar, K. Nederhoff, and A. Dastgheib. 2018. "Improving predictions of swash dynamics in XBeach: The role of groupiness and incident-band runup." *Coastal Engg Vol 134* 103-123.

Rosen, P.S. 1978. "A regional test of the Bruun Rule on shoreline erosion." *Marine Geoloty* V26 (1-2) M7-16.

Sayers, P., Li Yuanyuan, G. Galloway, E. Penning-Roswell, S. Fuxin, C. Yiwei, W. Kang, T. Le Quesne, L. Wang, and Y. Guan. 2013. "Flood Risk Management: A Strategic Approach." Online report, UNESCO, 202. doi:ISBN: 978-92-3-001159-8.

Shaw, J., R.B. Taylor, D.L. Forbes, M.-H. Ruz, and S. Solomon. 1998. *Sensitivity of the Coasts of Canada to Sea-Level Rise.* GSC Bulletin 505, Geological Survey of Canada.

Shrubsole, D., G. Brooks, R. Halliday, E. Haque, A. Kumar, J. Lacroix, H. Rasid, J. Rousselle, and S. Simonovic. 2003. *An assessment of flood risk management in Canada.* ICLR Research Paper 28, London, ON: Institute for Catastrophic Loss Reduction.

Slinn, D. 2008. *Wave setup methodology for the FEMA Mississippi Flood Study.* Supporting documentation for FEMA Mississippi Coastal Flood Hazard Project, Gainesville: U. Florida for FEMA.

Smit, P.,, M. Zijlema, and G., Stelling. 2013. "Depth-induced wave breaking in a non-hydrostatic, near-shore wave model." . *Coast. Engng.,* 76, 1-16.

Stedinger, J.R., R.M. Vogel, and E. Foufoula-Georgiou. 1993. "Frequency Analysis of Extreme Events, Chapt. 18." In *Handbook of Hydrology*, by D.R. Maindment. McGraw-Hill Book Co.

Stockdon, H.F., R.,A, Holman, P.A. Howd, and A.H. Sallenger. 2006. "Empirical parameterization of setup, swash and runup." *Coastal Engg (Elsevier)* 53 573-588.

Swail, V.R., V.J. Cardone, M. Ferguson, D.J. Gummer, E.L. Harris, E.A. Orelup, and A.T. Cox. 2006. "The MSC50 Wind and Wave Reanalysis." *9th International Workshop On Wave Hindcasting and Forecasting.* Victoria, BC.

Sweet, W.V., R.E. Kopp, C.P. Weaver, J. Obeysekera, R.M. Horton, E.R. Thieler, and C. Zervas. 2017. *Global and Regional Sea Level Rise Scenarios for the United States.* Technical Report NOS CO-OPS 083, NOAA.

Taylor, R.B. 2000. *A Re-examination of Beach Mining Along the Gasperaux Shore, Prince Edward Island.* Open File Report 3864, GSC (Atlantic), Dartmouth NS: Geological Survey of Canada .

The SWAN Team. 2009. *SWAN User Manual.* Delft, NL: Delft University of Technology.

Thieler, E.R., and E.S. Hammer-Klose. 1999. *National Assessment of Coastal Vulnerability to Sea-Level Rise: Preliminary Results for US Atlantic Coast.* Open File Report 99-593, Woods Hole, MA: US Geological Survey.

Thieler, E.R., O.H. Pilkey, R.S. Young, D.M. Bush, and F. Chai. 2000. "The use of mathematical models to predict beach behavior for US coastal engineering." *J. Coastal Research* 16(1) 48-70.

van der Meer, J.W., T. Bruce, J. De Rouck, A. Kortenhaus, T. Pullen, H. Schüttrumpf, P. Troch, and B. Zannutigh. 2018. *EurOtop - Manual on wave overtopping of sea defences and related structures 2nd Edition.* www.overtopping-manual.com. www.overtopping-manual.com.

van der Meer, J.W., W. Allsop, T. Bruce, J. de Rouck, T. Pullen, H. Schuttrumpf, P. Troch, and B. Zanuttigh. 2016. "Update of the EurOtop Manual: New insights on wave overtopping." *Coastal Engineering.* ASCE.

van Dongeran, A. 2018. "RISC-KIT: Resilience-increasing strategies for coasts - Toolkit." *Coastal Engg., Vol. 134* 1-254.

Van Gent, M.R.A, B. Pozueta, and H. Van den Boogaard. 2004. "Report on WP8: Prediction Method. Neural network modelling of wave overtopping. Deliverable D42 of European project CLASH (version 3)."

van Vuuren, D, J Edmonds, M Kainuma, K Riahi, A Thomson, K Hibbard, G Hurtt, et al. 2011. "The representative concentration pathways: an overview." *Climatic Change (2011) Vol. 109* 5–31.

Vogel, R.M., and A. Castellarin. 2017. "Risk, Reliability and Return Periods and Hydrologic Design, Chapter 78." In *Handbook of Hydrology*, by V.P. Singh, 78-1 to 78-10. McGraw Hill Book Co.

Wahl, T., and D.P. Chambers. 2015. "Evidence for multidecadal variability in US extreme sea level records." *J. Geophys. Res. Oceans, 120* 1527–1544, doi:10.1002/2014JC010443.

Webster, T. 2012. *Coastline change in Prince Edward Island, 1968-2010 and 2000-2010.* Project Report, Charlottetown: Atlantic Climate Adaptation Solutions Association.

Webster, T., and D. Stiff. 2008. "The prediction and mapping of coastal flood risk associated with storm surge events and long-term sea level changes." *Risk Analysis VI.* WIT Press. 129-138.

Webster, T., K. McGuigan, and C. Webster. 2011. *Survey grade GPS storm surge high water mapping.* Project Report, Charlottetown: Atlantic Climate Adaptation Solutions Association, 29.

Webster, T., K. McGuigan, K. Collins, and C. MacDonald. 2014. "Integrated river and coastal hydrodynamic flood risk mapping of the LaHave River estuary and Town of Briedgewater, Nova Scotia, Canada." *Water* Vol 6. www.mdpi.com/journal/water.

Williams, J., K. Horsburgh, J. Williams, and R.N.F. Proctor. 2016. "Tide and skew surge independence: New insights for flood risk." *AGU Geophysical Research Letters* 43: 6410-6417, doi:10.1002/2016GL069522.

Zhai, L., B. Greenan, J. Hunter, T. James, G. Han, R. Thomson, and P. MacAulay. 2014. *Estimating Sea-level Allowances for the Coasts of Canada and the Adjacent United States Using the Fifth Assessment Report of the IPCC; Canadian Technical Report of Hydrography and Ocean Sciences 300.* Dartmouth, NS: Fisheries and Oceans Canada.

Zhai, L., B. Greenan, J. Hunter, T.S. James, and G. Han. 2013. *Estimating Sea-Level Allowances for Atlantic Canada Under Conditions of Uncertain Sea-Level Rise.* Dartmouth, NX: Ocean and Ecosystem Sciences Division, Maritimes Region, DFO.

Zhang, H., and J. Sheng. 2013. "Estimation of extreme sea levels over the eastern continental shelf of North America." *j. Geophyical Research: Oceans* 118: 1-21.